Journal of Civil Engineering and Architecture Engineering

Volume No. 9

Issue No. 2

May - August 2025

ENRICHED PUBLICATIONS PVT. LTD

S-9, IInd FLOOR, MLU POCKET,
MANISH ABHINAV PLAZA-II, ABOVE FEDERAL BANK,
PLOT NO-5, SECTOR-5, DWARKA, NEW DELHI, INDIA-110075,
PHONE: - + (91)-(11)-47026006

Journal of Civil Engineering and Architecture Engineering

Aims and Scope

Journal of Civil Engineering and Architecture Engineering is a peer reviewed journal published by Original Papers. It is one of the pioneering starts up journal in Civil and Structural engineering which receives high quality research works from researchers across the globe. The journal publishes original research and review papers falling within the broad field of Civil Engineering.

Journal of Civil Engineering and Architecture Engineering

Journal of Civil Engineering and Architecture Engineering

(Volume No. 9, Issue No. 2, May - August 2025)

Contents

Turbulence over a Rough Bed using Double Averaged Navier-Stokes Equation

Santosh Kumar Singh[1]**, Koustuv Debnath**[2]

[1]*PhD Student, Indian Institute of Engineering Science & Technology, Shibpurs, Howrah-711103, India*

[2]*Professor, Indian Institute of engineering science & Technology, Shibpur, Howrah-711103, India*

Email: fmsks84@gmail.com

ABSTRACT

The paper describes an experimental study carried out in a laboratory flume to investigate the turbulence structure over cube mounted rough bed. The cubes were made of wood and were positioned at the channel bed with different relative spacing. The spacing was chosen such that roughness types under different spacing generally classified; isolated roughness flow, wake interference flow and skimming flow. The three-dimensional velocity field was measured by an Acoustic Doppler Velocimeter (ADV). The study particularly focuses on the changes induced in the spatially averaged mean velocity profile, turbulent intensity and Reynolds shear stress. The spatially averaged mean velocity profile show two distinct regions; the linear or exponential distribution below the roughness tops and logarithmic profile above the roughness top. Near the bottom, the form-induced stress changes significantly and then either decreasing or switching from making a negative to a positive with the roughness spacing.

Keywords: Roughness; Velocity; Spacing; ADV; Double-average

1. INTRODUCTION

The vast majority of environmental fluid flows are classified as hydraulically rough. This roughness may be both physical and biological. In essence this means that the influence of the bed roughness and local non-uniformity in the near-bed flow on the global flow characteristics cannot be ignored. These flows are typically described by the Reynolds averaged Navier-Stokes equations, which deal with time-averaged variables and involve no spatial averaging. Such an approach, however, is often inconvenient, due do the complex boundary conditions that lead to the high flow heterogeneity. The key drawbacks of the Reynolds averaged Navier-Stokes equations based approaches in relation to rough-bed flows have been discussed in Nikora et al. (2007a). It has been argued that to resolve the problem theoretically and conceptually, time averaging of the hydrodynamic equations should be supplemented by volume averaging or area averaging in the plane parallel to the mean bed surface. The double-averaging procedure gives new momentum for fluid, which are averaged in both time and space domains. Although the idea of spatial averaging has been used by many researchers (Smith and McLean, 1977; Wilson and Shaw 1977; Raupach et al. 1991 and others), the full development of this approach to use in hydraulics was fully made by Nikora et al. (2001, 2007a), who developed new continuity and momentum equations for rough-bed open channel flows by double-averaging the Navier-Stokes equations. The main advantages of this methodology, i.e. (a) self-consistency; (b) refined definitions for roughed flows such as flow uniformity, and the bed shear stress; (*c*) explicit accounting for the viscous drag, form drag and form-induced drag; e) scaling considerations and parameterizations based on double-averaged variables; and (f) partitioning of the roughness parameters and flow properties. These advantages use of the double averaged hydrodynamic equations helps in guiding and developing numerical models, designing laboratory field and experimental data analysis associated with rough-bed flows.

The spatial heterogeneity can contribute significantly to momentum transfer in the roughness layer it is not sufficient to consider Reynolds and viscous shearing alone; instead these should be complemented by the form-induced stress. In double-averaging terms, fluid stress therefore comprises three distinct com

$$\frac{\tau}{\rho} = \upsilon\left\langle \frac{\partial \bar{u}_i}{\partial x_j} \right\rangle - \left\langle \overline{u_i' u_j'} \right\rangle - \left\langle \tilde{u}_i \tilde{u}_j \right\rangle \tag{1}$$

$\upsilon\partial\langle\partial\bar{u}\rangle_i/\partial x_j$

where $(-\langle\overline{u_i'u_j'}\rangle)$ scous stress, which generally consider to be negligible, compared to spatially averaged Reynolds stress in rough turbulent flows, except in the immediate vicinity of the wall where velocity gradients are large.

The main objective of the present study is to investigate the effect of the superposition of surface waves of different frequencies on the flow over artificial rough bed using spatial averaging method. At first the double-averaged Navier-Stokes equations are presented as theoretical frame work for the whole analysis. The deviations of double average mean velocity, turbulent intensity, Reynolds shear stress, form induced stress and total stress over rough bed are investigated. This study also addresses the effect on turbulence properties due change in relative roughness spacing in context of double averaging. The spacing is chosen such that the three roughness types, isolated roughness flow (L/h = 9), wake interference flow (L/h = 5) and skimming flow (L/h = 3) are investigated. The investigators are affirmative that the quantitative knowledge generated in the present study will be useful for numerical modeling or laboratory investigations, environmental hydraulics of rough bed flows, and in understanding sediment pickup, grain-sorting and transportation under coastal environment in the cubical

2. Experimental program and Data analysis

Experiments were conducted in a laboratory flume at the Fluid Mechanics and Hydraulic Laboratory (FMHL) of Indian Institute of Engineering Science and Technology (IIEST), Shibpur, India. A specially designed flat bed open-channel flume of dimension 18.3 m long, 0.90 m wide and 0.90 m deep with a constant slope of 0.00025 was used for the experiments. The flat surface of the flume was finished with plane net cement, which was somewhat frictionless. Water was re-circulated into the flume by a vertical turbine pump of 0.30 m^3/s capacity from a sump of dimension 30 m long, 3 m wide and 2 m deep. The discharge into the flume was controlled by a control valve. The discharge valve was gradually opened to achieve desired discharge and the tail gate was operated simultaneously to ensure the desired flow depth (H). The water flow after the discharge from pump passed through series of wire-meshes placed at the upstream end of the flume to ensure the smooth and vortex free uniform flow through the experimental channel.

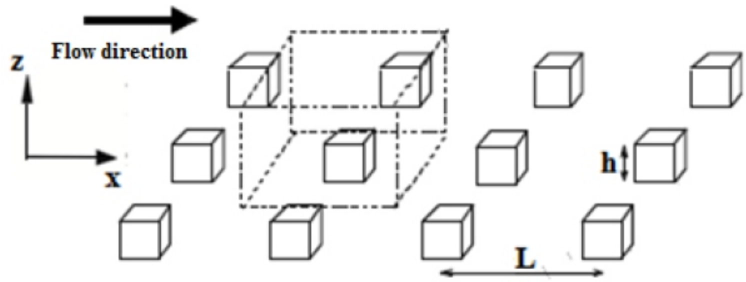

Figure 1. Cube arrangement in the experiment and calculation of domain

To perform experiments, the rough bed was established using large number of artificial water resistance wooden cube of dimension 0.025 m width × 0.025 m length × 0.025 m height. The cubes were polished to eliminate any excess material and to smoothen the exterior surface. The cubes were positioned along the flume (Fig. 1) using a special quality of adhesive (water resistance). Three different values of pitch length L (centre to centre spacing between two consecutive cubes) were chosen to achieve isolated roughness flow, wake interference flow and skimming flow (Perry et al. 1969). The cubical roughnesses were equally spaced along lateral and longitudinal direction so that the flow pattern repeats along the flume bed (Fig. 1). In this paper we consider the time-averaged flow variables do not change in time and the spatially-averaged flow variables change neither in the longitudinal direction nor in the lateral direction. Consequently, the spatially averaged bottom-normal and lateral velocities are equal to zero. Two different tests were carried out in the present study: (1) test over the flat surface, and (2) tests over the cubical roughness mounted on the flat surface at varying spacing. All experiments were conducted at location x = 12 m from the flume entrance where the flow was verified to be fully developed. The velocity data were collected at the rate of 40 Hz for 5 min duration for each measuring point with lowest each profile being 0.42 cm above the flat surface. Although it would have been preferable to sample even closer to the flat surface, initial test at closer distance gave noise with poor signal correlations. The increase in noise was likely due to echo effects from flat surfaced and high velocity gradients within the sampling volume (Lacey and Rennie 2012). In the present study, the raw ADV data were processed to remove these noises. These noises were removed by a phase space threshold despiking method described by Goring and Nikora (2002) and implemented in the Win-ADV software (Wahl 2000). To remove such effects, the velocity data collected by ADV were analysed systematically for all selected verticals. Assessment of the quality of individual time series velocity data is based on visual inspection of plotted raw velocity time series. The ADV velocity data were cleaned by removing all communication errors, low signal-to-noise ratio data (< 15 dB) and low correlation samples (< 70%). This was performed by Win-ADV software resulted in the removal of approximately 2% of all collected raw velocity time series. Such excluded signals were replaced by data using a cubic polynomial interpolation method. The effects of large noise were removed by minimizing the possible aliasing effect near the Nyquist frequency (herein $f_n = 20$ Hz). The highest measurement point from the bed was about 14 cm above the flume bed for each experiment.

The mean flow depth H was kept constant at 20 cm for all tests. All experiments were performed at single turbulent flow of flow rate (Q) = 0.053 m^3/s, at Reynolds number (Re = Uh/v = 58800, and Froude number $(Fr = U/\sqrt{gh})$ = 0.21, where U = 29.4 cm/s is the depth averaged velocity, v is the kinematic viscosity of water, and g is the acceleration due to gravity. All tests were fully rough turbulent flow of h/λ > 70, where $\lambda(=\upsilon/u_s)$ is the viscous length scale.

Table 1. Hydrodynamic Conditions

Reynolds number, $R_e(=Uh/\nu)$	58800
Depth average stream-wise velocity, U (cm/sec)	29.4
Mean flow depth, H (cm)	20
Froude number, $Fr(=U/\sqrt{gh})$	0.21
Friction velocity, $u_s\left(=\sqrt{\langle\tau_0\rangle/\rho}\right)$ (cm/sec)	2.0 (L/h = 3), 2.1 (L/h = 5) & 1.5 (L/h = 9)

3. Results and discussions

3.1 Experiment over the flat surface

In turbulent flow, the time-averaged mean velocities ($\overline{u},\overline{w}$), the root-mean-square velocity components (σ_u,σ_w) and the time-averaged Reynolds shear stress at each measuring point were computed by standard procedure (Nezu and Rodi 1986, Debnath et al 2012). For ease of comparison we have normalized the time averaged mean velocity, turbulent intensities and Reynolds shear stress by the friction velocity (u_*) and are given by

$$\hat{u} = \overline{u} / u_* , \hat{w} = \overline{w} / u_* \; I_u = \sigma_u / u_* , I_w = \sigma_w / u_* \text{ and } uw^+ = \overline{u'w'} / u_*^2 \tag{2}$$

The normalized mean velocity components ($\hat{u} = \overline{u} / u_*$, $\hat{w} = \overline{w} / u_*$), stream-wise turbulence intensity (I_u), bottom-normal turbulence intensity (I_w) and Reynolds shear stress (uw^+) over the flat surface are plotted all together in Figs. 3(a-d). The friction velocity (u_* = 1.47 cm/sec) is calculated from the universal velocity logarithmic law (Schlichting 1960) over the plane bed surface as

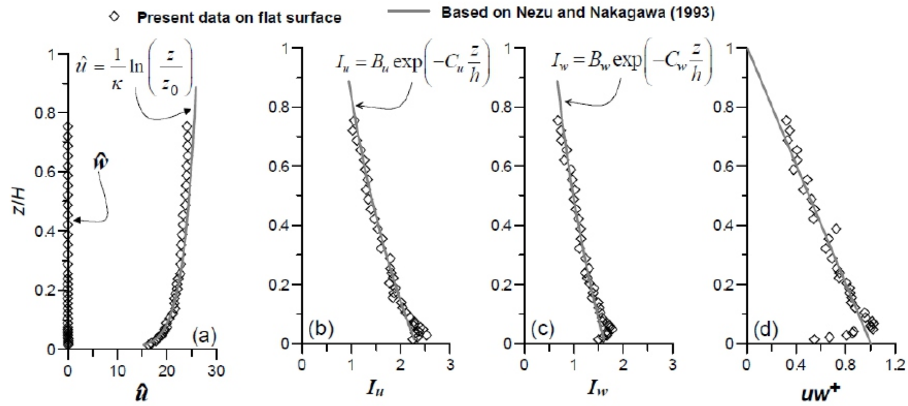

Figure 2. Normalized profile of (a) Stream-wise and bottom-normal mean velocities ($\hat{u}$ and $\hat{w}$), (b) Stream-wise turbulence intensity (I_u), (c) Bottom-normal turbulence intensity (I_w) (d) Reynolds shear stress (uw^+), based on present measurements on flat surface. Here the parameters B_u = 2.5, B_w = 1.61, C_u = 1.01 and C_w = 0.98.

$$\hat{u} = 1 / \kappa \ln(z / z_0) \tag{3}$$

where k (= 0.4) is the von Karman constant and z_0 (= 0.0014 cm) is the equivalent bed roughness with coefficient of regression $R^2 \approx 0.96$. It is also observed that the vertical and the lateral mean velocity components are zero throughout the depth of the flow (Fig. 2a). The Reynolds shear stress component (Fig. 2d) exhibits the same features as seen in the turbulent intensity profile. It observed that Reynolds shear stress increases and reaches a maximum value at a distance close to the bed and then decreases towards the free surface. The results on flat surface are in good agreement with Nezu and Rodi (1986) and Nezu and Nakagawa (1993).

3.2 Experiment over cube mounted bed

3.2.1 Mean velocity

Our results support a composite profile consisting of two theoretical distributions: the linear or exponential distribution below the roughness tops (z_c), and logarithmic law above the roughness top.

The Fig. 3 displays the double-averaged velocity profile $\langle \hat{u} \rangle = (\langle \overline{u} \rangle / u_s)$ normalized by spatially averaged friction velocity $u_s \left(= \sqrt{\langle \tau_0 \rangle / \rho}\right)$ against normalized vertical distance (*z-d*)/*h*, where *d* is the zero-plane displacement. The methodology adopted for estimation of the zero plane displacement is shown later. The value of u_s are determined from the spatially averaged bottom shear stress $\langle \tau_0 \rangle$. The spatially averaged bottom shear stress is determined by extrapolating the spatially averaged Reynolds shear stress profile up to the roughness top.

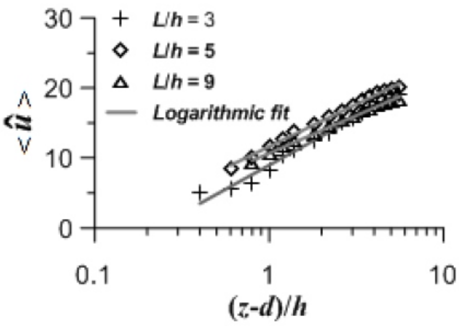

Figure3. Logarithmic representation of above roughness top against (*z-d*)/*h* for (a) *L*/*h* = 3, (b) *L*/*h* = 5 and (c) *L*/*h* = 9

Figs.3a-c presents results for relative roughness spacing (*L*/*h*) = 3, 5 and 9 respectively. The vertical distribution of $\langle \hat{u} \rangle$ for flow over cubic roughness follow the logarithmic behavior above roughness tops with coefficient of regression $R^2 \approx 0.95$ for all the relative spacing. This result seems to confirm the findings of Coleman et al. (2007).

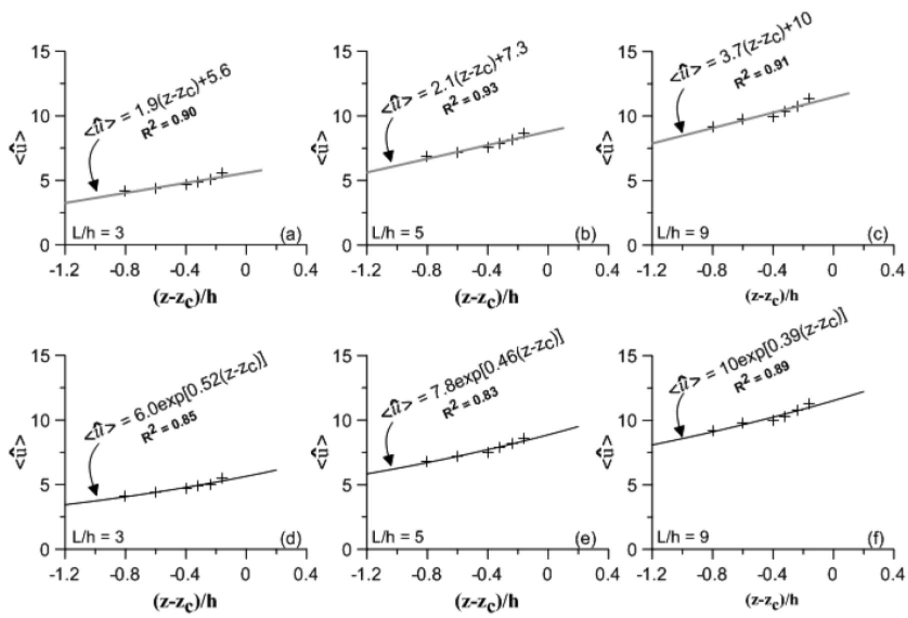

Figure 4. Linear (a-c) and exponential (d-f) double average velocity distribution below the roughness top for relative roughness spacing's *L*/*h* = 3, *L*/*h* = 5 and *L*/*h* = 9.

Fig. 4 shows the linear and exponential distributions below the roughness top for different relative roughness spacing (L/h = 3, 5 and 9). For comparison of model suitability, both plots (linear and exponential) included the same number of data points up to 5 mm above the roughness tops ($0 < (z-z_c)/h \leq 0.2$). Below the roughness layer or roughness crest (z_c) the linear distribution described the data (coefficient of regression $((R^2)_{L/h = 3,\ 5\ \text{and}\ 9} \approx 0.90$, 0.93 and 0.91) better than the exponential distribution $((R^2)_{L/h = 3,\ 5\ \text{and}\ 9} \approx 0.85$, 0.83 and 0.89). Nikora et al. (2002) propose that the double averaged velocity profiles can take several forms (constant, exponential, linear or a combination of these) dependent on flow conditions and roughness geometry.

Coleman et al. (2006) found linear profile and linear to slightly exponential form for fluvial sand waves of $L/h = 20$ and $L/h = 10$ respectively. Coleman et al. (2007) found an exponential profile (below the roughness crest) for the closely spaced ribs ($L/h < 10$), and a linear profile for the widely spaced ribs ($L/h \geq 10$), with the profile transitioning between the two for increasing L/h. The present results shows good fit to linear profile below the roughness tops compared to exponential for all the three spacing. This is in contradictory to the observation by Bose and Dey (2007); they reported a second-degree polynomial distribution below the roughness top. However the present results are in conformity with Raupach et al. (1991) with $R^2 \approx 0.85$ for closer or dense roughness spacing.

3.2.2 Zero-plane displacement height (d)

In order to find the zero-plane displacement height we used the method suggested by Nikora et al. (2002). They calculated d for various types of roughness and flow conditions and the results showed that the position of the zero-plane goes up with increasing roughness density. We can write the law of wall for flow field in its general form with zero-plane displacement (d) as follow:

$$\frac{\langle \overline{u} \rangle}{u_s} = \frac{1}{k} \ln \frac{z-d}{z_0} \tag{4}$$

where $\langle \overline{u} \rangle$ the spatially averaged velocity, k is the von Karman constant, z_0 is the roughness length, and $u_s \left(= \sqrt{\langle \tau_0 \rangle / \rho} \right)$ is the friction velocity. The zero-plane position is evaluated by the method based on the inverse of the velocity profile derivative suggested in Nikora et al. (2002).

Differentiating equation (4) with respect to z we get

$$\frac{d\langle \overline{u} \rangle}{dz} = \frac{u_s}{k(z-d)} \tag{5}$$

After rearranging equation (5), we can write

$$\left(\frac{d\langle\overline{u}\rangle}{dz}\right)^{-1} = \frac{k}{u_s}z - \frac{k}{u_s}d = a_1 z - b_1 \tag{6}$$

where a_1 and b_1 are the coefficients of linear fit to the inverse velocity gradient. Then, the displacement height is evaluated as $d = b_1/a_1$ and it is adjusted to give $k = 0.4$

The left hand side of the equation (6) represents the ratio of the mixing length l_e to the friction velocity u_s i.e., $\left(d\langle\overline{u}\rangle/dz\right)^{-1} = l_e(z)/u_s$. Therefore, plots of spatially averaged inverse velocity gradient may be interpreted as vertical distributions of the mixing length (l_e) normalized with shear velocity. The distributions of double average velocities were smoothed by using a two-point running mean in the vertical before calculations of velocity derivatives. Fig. 5 provides the plot of $\left(d\langle\overline{u}\rangle/dz\right)^{-1}$ for different L/h against z.

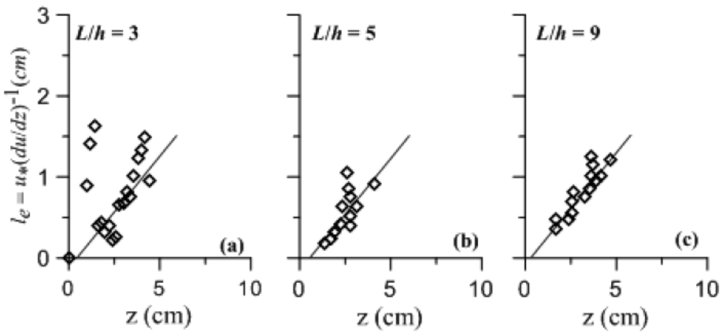

Figure 5. Determination of the zero-plane height *d* (using Eq. 6) for (a) $L/h = 3$, (b) $L/h = 5$ and (c) $L/h = 9$. The solid line represents the linear fit to the straight line part of the profile.

The variations in zero-plane displacement (d) with L/h for only current and combined current and wave with frequency $f = 1$ Hz and $f = 2$ Hz is shown in Fig.6. The value of d decreases with increasing relative roughness spacing (L/h) which is consistent with the findings of Coleman et al (2007) for $L/h = 3$ and 5. However the present results of d differ from the findings of Coleman et al. (2007) for $L/h > 5$. This is probably because the positions of d depend on roughness density, geometry and energy of large eddies (Manes et al. 2007).

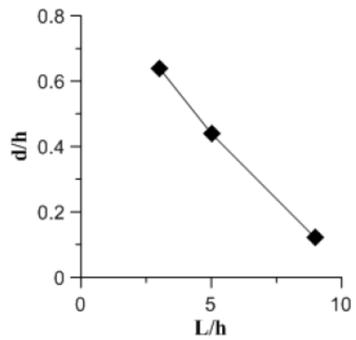

Figure 6. Variation of non-dimensional zero-plane displacement d/h against L/h (using Eq. 6)

3.2.3 Spatially averaged total shear stresses

The spatially averaged total shear stress was obtained by same procedure as discuss in Manes et al. (2007) i.e., by the addition of the spatially averaged Reynolds shear stress $\langle \overline{u'w'} \rangle$, the form-induced shear-stresses $\langle \tilde{u}\tilde{w} \rangle$, and the viscous shear stress $\upsilon\partial\langle \overline{u} \rangle/\partial z$. The spatially averaged total shear stress $\langle \tau_t \rangle$ is balanced by the gravity and has to have a linear profile (Mannes et al. 2007). Therefore to check the linearity of the total shear stress we have performed the analysis above and below the roughness top. All vertical distribution of shear stress components (τ) $(=\langle \tau_t \rangle, \langle \overline{u'w'} \rangle, \langle \tilde{u}\tilde{w} \rangle$, and $\upsilon\partial\langle \overline{u} \rangle/\partial z)$ are plotted in Fig. 13 against z/h for relative spacing $L/h = 3$ (Fig.7a), $L/h = 5$ (Fig.7b) and $L/h = 9$ (Fig.7c).

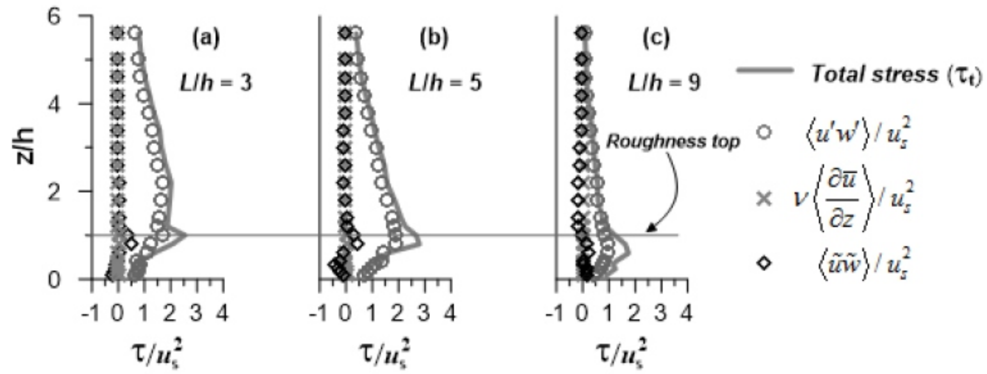

Figure 7. Normalized vertical distribution of shear stress components against z/h for (a) $L/h = 3$, (b) $L/h = 5$ and (c) $L/h = 9$

In all experiments the spatially-averaged Reynolds shear stress profile is linear above the roughness layer ($z/h > 1.2$) as observed for time averaged profiles over plane bed (Nezu and Nakagawa 1993). Fig. 7 shows that the double averaged Reynolds shear stress is the main dominating flow stress throughout the flow depth except below the roughness top probably due to decrease in turbulence level below the roughness top. The changes in peak position of spatially averaged Reynolds shear stress strongly depend on relative roughness spacing. The form-induced stress arises from the correlations between point-to-point spatial deviations in time-averaged velocity components, the form-induced velocities $\tilde{u}$ and $\tilde{w}$. It therefore depends on both the spatial coherence and magnitude of spatial variance in the time-averaged flow. Form-induced stresses are essentially zero above the roughness layer, and increase to a positive peak below the roughness top ($z/h = 0.8$), this peak decreasing for increasing roughness spacing. Below the roughness top where the mean flow is highly non-homogeneous, the decrease of $\langle \overline{u'w'} \rangle$ is compensated for by the appearance of $\langle \tilde{u}\tilde{w} \rangle$ and by the viscous shear stress $\upsilon\partial\langle \overline{u} \rangle/\partial z$ which have approximately same magnitude above the roughness tops for all the conditions. Below the roughness top the $\langle \tilde{u}\tilde{w} \rangle$ and $\langle \overline{u'w'} \rangle$ have comparable magnitude, whereas the viscous stress becomes negligible throughout depth for all conditions. Above the roughness top, the spatially averaged total shear stress ($\langle \tau_t \rangle$) reasonably follows

4. Conclusions

The purpose of the present study was to ascertain the effect of double-averaged parameters on the flow over cubical roughness with different relative spacing. An ADV was used to collect the velocity data over a single roughness wavelength. Three different values of pitch length (L) were use to achieve isolated roughness flow, wake interference flow and skimming flow. The cubical roughnesses were equally spaced along lateral and longitudinal direction so that the flow pattern repeats along the flume bed and it was assumed that, all averaged quantities do not vary in the flow direction. The effect of roughness spacing on the spatially averaged mean velocities and total stress containing Reynolds shear stress, form-induced stress and viscous stress in an open channel flow has been presented in this paper as a function of relative roughness spacing. The finding reveals that stream-wise double averaged profiles were support a composite profile consisting of two theoretical distributions: the linear or exponential distribution below the roughness tops and logarithmic law above the roughness top. The form-induced stress which is calculated from spatially averaged velocity components. Near the bottom the form-induced stress changes significantly and then either decreasing or switching from making a negative to a positive with the roughness spacing. Above the roughness top, the spatially averaged total shear stress reasonably follows the expected linear shear stress profile for all the experimental conditions.

This study could provide a better understanding of turbulence over a cubical roughness with different relative spacing. It is of future interest to improve our understanding of turbulence with widely varying roughness spacing. Detailed investigations are important to formulate a better modeling of three-dimensional flow structure which will help the researcher to understand the mean flow and turbulent statistics in the field of hydraulic.

5. Reference

- *Agelinchaab, M., and Tachie, M, F., (2006). "Open channel turbulent flow over hemispherical ribs". J. Heat, Fluid Flow, 27, 1010-1027.*
- *Bose, S.K., Dey, S., (2007) "Curvilinear flow profiles based on Reynolds averaging." Journal of Hydraulic Engineering, ASCE, 133(9):1074–1079.*
- *Coleman, S.E., Nikora, V.I., McLean, S.R., and Schlicke, E., (2007). "Spatially averaged turbulent flow over square ribs" J. Eng. Mech., ASCE, 123, 194-204.*
- *Coleman, S., E., Nikora, V., I., McLean, S.R., Clunie, T., M.,Schlicke, T., and Melville, B., W., (2006). Equilibrium hydrodynamics concept for developing dunes. Phys. Fluids, 18(10), 105104, 1-12.*
- *Cooper, James R., Aberle, J., Koll, Katinka., and Tait, Simon J. (2013). Influence of relative submergence on spatial variance and form-induced stress of gravel-bed flows. Water Resour. Res., 49, 1-13.*
- *Debnath, K., Manik. M., K., and Mazumder, B., S., (2012). Turbulence statistic of flow over scoured cohesive sediment bed around circular cylinder." Adv. Water Resour., 41, 18–28.*
- *Goring, D., G., and Nikora, V. I., (2002). Despiking acoustic Doppler velocimeter data. J. Hydraul. Eng., ASCE, New York, 128(1), 117–126.*
- *Lacey, R., W., J., and Rennie, D. C., (2012). Laboratory investigation of turbulent flow structure around a bed mounted cube at multiple flow stages. J. Hydraul. Eng., ASCE, New York, 138, 71–83.*

- *Manes, C., Pokrajac, D., and McEwan, I., (2007). Double-averaged open channel flows with small relative submergence. J. Hydraul. Eng., 133(8), 896-904.*
- *Nezu, I., and Nakagawa, H., (1993). Turbulence in Open-Channel Flows." A. A. Balkema, CRC Press, Rotterdam.*
- *Nezu, I., and Rodi, W., (1986). Open-channel measurement with a laser Doppler anemometer. J. Hydraul. Eng., ASCE, New York, 112(5), 335-355*
- *Nikora, V. I., Goring, D., McEwan, I., and Griffiths, G., (2001). Spatially averaged open-channel flow over rough bed. J. Hydraul. Eng., ASCE, 127(2), 123-133.*
- *Nikora, V., Koll, K., McLean, S., Dittrich, A., and Aberle, J., (2002). Zero-plane displacement for rough-bed open-channel flows. Proc., Int. Conf. on Fluvial Hydraulics, River Flow 2002, Louvain-la-Neuve, Belgium, September 4-6, Taylor and Francis, London, 83-92.*
- *Nikora, V.I., McLean, S. R., Coleman, S. E., Pokrajac, D., McEwan, I., Campbell, L., Aberle, J., Clunie, T. M., and Koll, K., (2007a). Double-averaging concept for rough-bed open-channel and overland flows: Application. J. Hydraul. Eng., ASCE, 133(8), 884-895.*
- *Raupach, M. R., Antonia, R. A., and Rajagopalan, S., (1991). Rough wall turbulent boundary layers. Appl. Mech. Rev., ASME, 44(1), 1-25.*
- *Schlicting, H., (1960). Boundary layer theory. 4th Edition New York: McGraw Hill.*
- *Smith, J. D., and McLean, S. R., (1977). Spatially averaged flow over a wavy surface. J. Geophys. Res., 82(12):1735–1746.*
- *Wahl, T. L., (2000). Analyzing ADV data using WinADV, in Building Partnerships, edited by R. H. Hotchkiss and M. Glade, sect. 75, chap. 3, Am. Soc. Civ. Eng.*
- *Wilson, N. R., and Shaw R. H., (1977). A higher order closure model for canopy flow. J. Applied Meteorol., 16, 1197-1205.*

Rejuvenation of Bisaindha Tank Project

Vishnu Arya
Madhya Pradesh Water Resources Department

ABSTRACT

In India, tanks/ponds and lakes have traditionally played an important role in conserving water for meeting various needs of the communities. As per 3rd Minor Irrigation Census 2000-2001 , there are 5.56 lakhs tanks and storages in the country as minor irrigation sources, creating 6.27 million hectares of irrigation potential. Out of 5.56 lakhs tanks, 4.71 lakhs tanks are in use, and remaining 0.85 lakhs tanks are not in use for one reason or the other, as a result of which one million hectares of irrigation potential has been lost.

However, many of these water bodies have gone into disuse because of the development of ground water irrigation system, inadequate maintenance, encroachments, illegal diversion of land for construction purposes etc. A pilot scheme for "Repair, Renovation and Restoration (RRR) of Water Bodies" directly linked to agriculture was launched in January 2005 for implementation during the remaining period of Xth plan with an outlay of Rs 3000 crores. The scheme was sanctioned in respect of 1098 water bodies in 26 districts of 15 states with a target to create 0.78 lakh hectares additional irrigation potential. Bisaindha Tank Project in district Sidhi (M.P.) is one of them.

Bisaindha Tank Project was constructed in the year 1992 with culturable command area of 1056 hectares, but the actual average irrigation for the last five years is only 630 hectares, which clearly indicates the difference between irrigation potential created and irrigation potential utilised. The reason being seepage loss and siltation of earthen canal due to which about 80 hectares agricultural land is water logged. It is proposed that the earthen canal should be lined to create 120 hectares of additional irrigation potential and the water logged area should be reclaimed.

The live storage capacity of Bisaindha Tank is 5.98 million cubic meters but due to collapse of boulder toe and seepage drains, live storage capacity has been reduced considerably. It is proposed to reconstruct the boulder toe and repair the seepage drains to save the precious and scarce irrigation water.

Results indicates that the methodology can be extended to other similar situations.

Keywords: RRR, boulder toe, seepage drains.

1. SALIENT FEATURES

1. Name of Scheme: Bisaindha Tank Project
2. District : Sidhi
3. Tahsil : Gopad Banas
4. Location :
   (a) Village : Bisaindha
   (b) Toposheet No.: 63H/15
   © Longitude : $81^0 56' 00''$
   (d) Latitude : $24^0 23' 00''$
5. Name of river/ stream : Local Nalla
6. Year of completion : 1992
7. Benefits:
   (a) Culturable command area : 1006 hectares
   (b) Designed irrigation : Kharif-777 hectares, Rabi- 227 hectares
   (c) Additional rabi irrigation after rejuvenation : 227 hectares

2. RESREVOIR DATA

1. Catchment Area:15.61 square kilometres
2. Live storage capacity: 5.95 million cubic meters

3. PRINCIPAL LEVELS OF DAM

1 River bed level : RL 97.54 m

2 Low sill level: RL 104.00m

3 Full reservoir level: RL 113.75 m

4 Maximum water level :115.25 m

5 Free board : 1.8 m

4. DAM DATA

1. Type of dam : Earthen/ Homogeneous
2. Length at top : 141 m
3. Top width : 6.0 m
4. Maximum height : 23.50 m

5. CANAL DATA

1. Length: main canal-7.2 kilometers, minor/ sub-minors -28 kilometers
2. Discharge at head : 1.0 cumecs
3. Thickness of lining :0.06 m
4. Average depth of silt to be removed : 0.45 m

6. ACTUAL IRRIGATION

2009-10	:	142 hectares
2010-11	:	168 hectares
2011-12	:	637 hectares
2012-13	:	627 hectares
2013-14	:	661 hectares

7. BOULDER TOE

Since height of embankment dam is more than 15m, as per technical circular 40 of Madhya Pradesh Water Resources Departmet, boulder toe has been provided in the entire reach of dam with a height of H/5 and separated from casing material and base material by filter layer.

The filter criteria is:

D_{15} of filter /D_{85} of filter < 5

D_{15} of filter/ D_{15} of filter <20 but >4

D_{50} of filter/ D_{50} of filter < 25

Filter will extend for full length between d/s hearting toe or imaginary hearting toe with 1:1 slope.

Due to aging and /or deferred maintenance , the boulder toe has been damaged and muddy water is seen on the downstream of toe. Hence it is proposed to reconstruct the boulder toe.

8. LEAKAGE/ SEEPAGE DRAINS

In designing an earth dam, the safety of the bund requires that whatever water leaks through thr hearting material should drop towards the ground in as rapid a slope as possible, so that the hydraulic gradient does not come near the other slope of the dam. The weakest point in the dam is its toe. If the foundation soil under the bund near the toe or the ground just outside the toe becomes wet, there is a danger of the foundation soil being squeezed out from under the bund. The foundation soil has not only resist a vertical pressure but also horizontal thrust. It is therefore, necessary that the foundation under the outer casing should be kept as dry as possible and this is achieved by providing leakage drains under the outer casing to receive leakage(seepage) water, and carry it off outside the bund as rapidly as possible.

In the present case the seepage drains has been damaged. It is proposed to provide 90cmx90cm size seepage drains below the filter and it will have a filter all around.

8. PITCHING/RIP-RAP

The term pitching refers to the roughly squared masonry or precast blocks or embedded stones laid in regular fashion with dry or filled joints, on the upstream slope of an embankment dam or on reservoir shore to provide protection to the embankment materials against erosion due to wave action etc. and also to give pleasing appearance.

Provision of filter under rip-rap prevents the waves generated in the reservoir, from eroding and washing out the underlying embankment material.Since the rip-rap is generally poorly graded due to predominance of one size material, the provision of adequate filter of the fine and cource material is also essential.

In the present case the pitching has been disturbed, hence it is proposed to repair the same. The thickness of rip-rap depends upon the maximum wave height . It shall in no case be less than 300 mm.

9. LINING OF CANAL

To minimise the conveyance loss and to conserve water and land resources, it would be ideal to plan, design and construct the canal system in irrigation projects as lined system down to 5-8 hectares sub-chaks.

At present the canals of Bisaindha Tank Project is unlined with a head discharge of one cumecs. The base width is 2.8 m and depth is 0.8 m with a free-board of 0.45 m. the length of main canal is 7.2 kilometers and side slope is 2:1, which is proposed to be lined with concrete of 0.06 m thickness. Benefit/cost ratio is worked out to be more than unity.

After lining , precious and scarce irrigation water will be saved and water logged area should be reclaimed which may be used for agriculture purpose.

10. UNCERTAINITY OF COST EFFECTIVENESS OF LINING

Inspite of the fact that extensive effort have so for been carried out in India and abroad including developed countries like USA, to economise on lining of canal system; the answer to cost effectiveness of lining a canal system still remains questionable due to various factors indicated hereunder:

1. It is difficult to generalise the extent of losses taking place in different limbs of canal system (main/branch canal, distributaries, minor, sub-minors and water course and /or field channels) because it depends upon the size and shape of the project, topography, surface conditions , environmental conditions, cropping patterns etc. Thus, it defers from project to project.
2. Data available in some projects in USA indicates that earthen embankment if well compacted can control seepage to considerable extent. The fact however is still to be established through long term observations under different conditions on several unlined system.
3. Percentage reduction in seepage by lining is much less what is normally assumed in the formulation of the project.
4. The advantage of reduced maintenance claimed in favour of lining does not appear to accrue in practice in the long run.
5. Although, theoretically, there is reduction in rugosity co-efficient initially due to lining over a period of years, it increases due to weed growth and vegetation, off setting to some extent the initial advantage.
6. The seepage loss through a canal system is not a total loss of water. A major portion of it forms a part of rechargeable ground water which can again be used for irrigation.

However, there are many direct and indirect benefits of lining , which can not be ignored.

11. RESULTS

After rejuvenation of Bisaindha Tank Project, following objectives have been achieved:

1. Comprehensive improvement and restoration of water body thereby increasing tank storage capacity.
2. Ground water recharge.
3. Increased availability of drinking water.
4. Improvement in agriculture/horticulture productivity.
5. Community participation and self supporting system for sustainability of water body.

12. CONCLUSION

Based on availability/limited data ,an attempt is made to rejuvenation of water body. Results indicated that the methodology can be extended to other similar situations.

13. REFERENCES

Technical circulars of Madhya Pradesh Water Resources Department.

ACKNOWLEDGEMENT

Author is thankful to the Madhya Pradesh Water Resource Department for providing encouragement to carry out the task.

Numerical Investigation of Dam Break Problem in Flat Bed Reservoir

Parvathy G. Panicker[1], Arun Goel[2], Hareesh R. Iyer[3]

[1] *M.Tech student, Civil Engineering Department, NIT Kurukshetra, Kurukshetra, 136119, India*
parvathygpanicker@gmail.com, +918943434701

[2] *Professor, Civil Engineering Department, NIT Kurukshetra, Haryana, 136119, India*
drarun_goel@yahoo.co.in, +91941639419

[3]*Assistant Professor, Mechanical Engineering Department, Marian Engineering College, Kerala, India*
hareeshriyer@hotmail.com, +919846519139

A B S T R A C T

Impact of one-dimensional impulse waves on a downstream wall following a dam break has been studied using VOF method. The wave velocity and wave amplitudes are analyzed by changing the drop height of the upstream dam break model and length of the downstream reservoir. Free-surface elevations (wave amplitude), wave velocity etc in the lower reservoir, before and after upstream dam collapse are monitored for a time period of 10 sec using ANSYS FLUENT. The bed of the reservoir where the wave traverses is considered flat and mildly rough. Shallow water theory and shallow water equations (SWE) are not applicable as the water catchment in the reservoir is sufficiently deep. The behavior of impacting wave front from the initiation of wave through its transformation and damping out are closely monitored for the non-sloping bed and it was found that for the same drop height, the bed roughness and bed length governed the wave rise and travel. This flat-bed condition serves to analyze the effect of energy transfer from the dam break into the wave generation. The parameters are non-dimensionalised for easier interpretation of the wave behavior.

Keywords: Dam Break, Volume of fluid method, impulse waves, run-up, Navier-Stokes solver

1. INTRODUCTION

The dam break problem has been of high research interest for the fluid mechanics and hydraulics community for decades for the variety it poses depending on the field of applications. Technically, dam break means, a constrained volume of water breaks its boundary and flows downstream, resulting in an unusual wave formation. The wave front formation can be due to earthquakes, landslides or other natural or artificial phenomenon. Wave run-up is a topic of high research interest in the past few decades. However, due to the many complicated features inherent to this problem such as breaking, air entrainment, turbulence etc., it is still not possible to describe the wave run-up accurately by means of any single method. The wave run-up associated with the impact on water retaining structures is a fluid-structure interaction (FSI) problem which is very complicated on one hand and a great challenge to the hydraulic and coastal engineers on the other hand.

The numerical simulation can be done in 2D and 3D using commercial dam break solvers and open-source programs. With the development of computational fluid dynamics (CFD), the dam break analysis gained more research interest [2]. This work uses ANSYS FLUENT [7] to simulate dam break which further evolves into a wave-impact problem. FLUENT employs the Eulerian Finite Volume Method wherein the unsteady form of Navier-Stokes equations is solved for the dam break analysis. Volume of Fluid (VOF) method tracks the free surface [3] which is adopted by FLUENT for simulations involving multiphase flow.

The present work attempts to develop a computational model of the dam break problem to the upstream of a flat bed reservoir. Upon dam break, an advancing wave front is generated and the scenario is simulated to study the wave behaviour. This paper primarily focuses on the variation of wave parameters in flat-bed reservoir considering different dam break drop heights and different bed lengths. The VOF method captures the open channel wave propagation from the initiation of the wave through its settling. The parameters of the flow model i.e. wave velocity and wave amplitude is compared to identify the variation of wave behaviour with respect to the geometry change in the reservoir. This problem can be studied with a variety of other parameters such as a sloping bed, shallow reservoir, continuous open-channel flow etc which are beyond the scope of the work. With the level of accuracy and capability of the available computational methods in solving such two phase problems, open-channel flow simulations can be performed satisfactorily even though marginal deviations from the experimental observations may be observed.

2. Problem formulation

The schematic representation of the dam break problem is given in Figure 1. A scaled model of an actual reservoir construction is considered here. In this model, the tank dimensions are L = 8 m, H = 5 m; the dimensions of the obstruction (dam cross section) downstream are top width, a = 0.3 m, bottom width, b = 0.45 m, dam height, h = 1.2 m, sill level, d = 1 m for the wave medium to be of considerable depth and the air-water phases being defined by volume fractions. For the sake of computational modelling, the benchmarked dam break problem is used. A water column is modelled at a higher elevation which collapses into the reservoir downstream to it due to gravity. Wave impact on the wall upstream of the lower dam is observed. The dam is located at a distance of 4.8 m from the origin. The bed slope is not considered in the model even though bed friction is considered.

The boundary conditions are also as shown in the Figure1. Wall boundary conditions are adopted for the direct water contact regions in the problem domain. Another study with a pressure outlet condition for the rightmost boundary showed the escape of spilled water in the downstream after wave impact. However, these results do not give the exact information on the amount of water over flown during wave impact. Free slip wall was defined for the lower dam cross section. The dam break model was defined at a convenient elevation from the basin of the lower reservoir such that water just spills over the dam top upon the upstream dam collapse and corresponding wave impact. The high Reynolds number observed characterizes the turbulence initiated by the dam break on to the water below. This condition symbolizes a real reservoir with water stored up to full reservoir level (FRL) experiencing a sudden rush of water from the upstream. The effect of turbulence is also considered to understand the capabilities of the NS solver to handle such complexities in the problem.

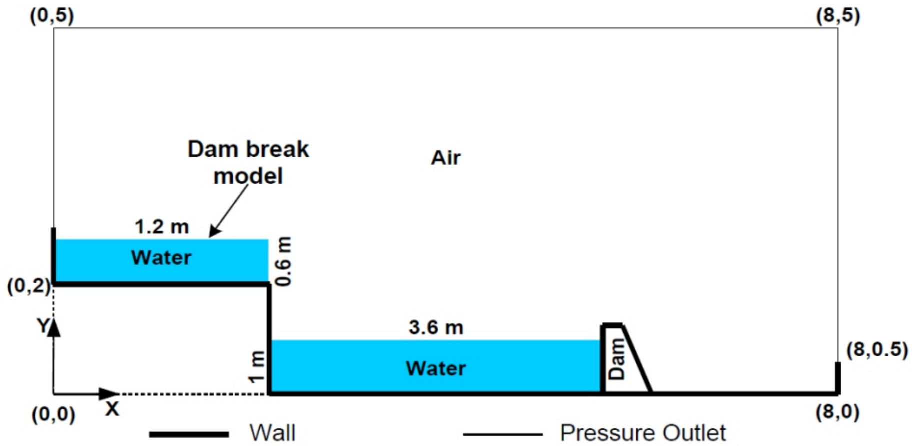

Figure 1 A schematic diagram of the dam break problem for flatbed reservoir

3. Governing equations

The momentum equations for the 2D mathematical model shown in Figure 1 are as follows

$$\frac{\partial u}{\partial t}+u\frac{\partial u}{\partial x}+v\frac{\partial v}{\partial y} = -\frac{1}{\rho}\frac{\partial P}{\partial x} \tag{1}$$

$$\frac{\partial v}{\partial t}+u\frac{\partial v}{\partial x}+v\frac{\partial v}{\partial y} = -\frac{1}{\rho}\frac{\partial P}{\partial y}-g \tag{2}$$

The flow field equations to be solved for the Eulerian mesh are the Navier-Stokes equations

$$\frac{\partial u}{\partial t}+u\frac{\partial u}{\partial x}+v\frac{\partial u}{\partial y} = -\frac{\partial P}{\partial x}+g_x+v\left[\frac{\partial^2 u}{\partial x^2}+\frac{\partial^2 u}{\partial y^2}\right] \quad 3$$

$$\frac{\partial v}{\partial t}+u\frac{\partial v}{\partial x}+v\frac{\partial v}{\partial y} = -\frac{\partial P}{\partial y}+g_y+v\left[\frac{\partial^2 v}{\partial x^2}+\frac{\partial^2 v}{\partial y^2}\right] \quad 4$$

where (u,v) is the velocity components in the Cartesian coordinates (x,y) and ν is the coefficient of kinematic viscosity. The incompressibility condition is defined by $\nabla\cdot\vec{u} = 0$. The wave phenomenon is characterized by the one dimensional wave equation mathematically expressed as

$$u_{tt} = c^2\, u_{xx} \quad 5$$

where u_{tt} and u_{xx} are the second temporal and spatial derivatives of velocity respectively.

4. Methodology

The drop height of the upper reservoir (the dam break model) was varied between 0.5 m and 1.5 m. Subsequently, for each varied drop height, the length of the lower reservoir was changed between 3.6 m and 6 m. Thus a combination of nine models was developed in the case of a flatbed downstream reservoir as shown in Table 1. Eulerian structured mesh was developed for all the problem models and wave transients were monitored for a time of 10 sec. The energy transport from a stored potential form to transient kinetics helps in the study of the impulse wave behaviour from the initiation through suppression. ANSYS FLUENT was used to simulate the dam break, resulting impact wave generation, wave transformation from impulse to bore and subsequent wave damping. Geo-reconstruct subfunction of VOF method tracks the free surface location during the wave travel.

Table 1 Numerical analysis matrix

Fall height (m)	Bed length (m)	Bed slope (°)	No. of models
0.5	3.6	0	3
	4.8		
	6.0		
1.0	3.6	0	3
	4.8		
	6.0		
1.5	3.6	0	3
	4.8		
	6.0		

5. Results and discussions

As indicated in Table 1, three models of varying bed lengths for each specific drop height were simulated. The drop heights for the wave generation model were set to 0.5 m, 1.0 m and 1.5 m. For each drop height, the time of initiation of waves in the respective models remained a constant, irrespective of the bed length or bed slope.

In the 0.5 m drop height category, the maximum non-dimensionalized wave height (*h/H),* commonly referred as wave height parameter, developed is 1.252 where *H* is taken as 1.0 m, the initial water depth, for all the cases. Also the maximum wave height in these three models immediately after the impulses was observed at about the time parameter value of 2.82. In these three models, the location of maximum wave height immediately after impulse was observed at about 2.54 m from the leftmost wall. Figure 2 shows the maximum wave heights observed in this category of drop height.

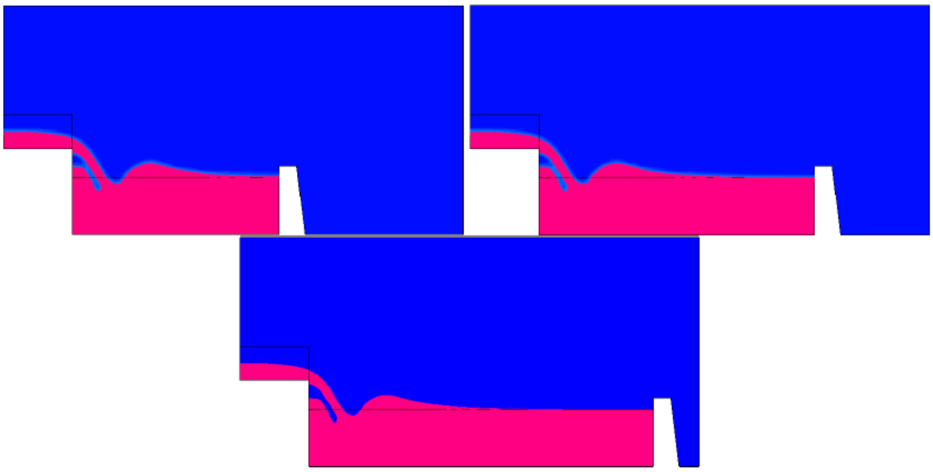

Figure 2. Maximum wave heights observed from the 0.5 m drop height category for the three bed lengths after the wave originates

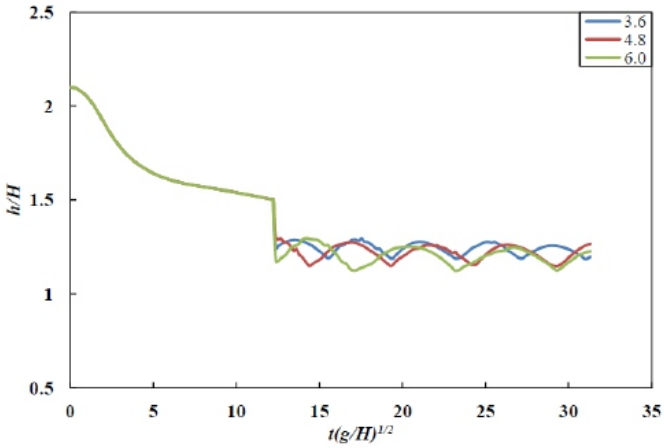

Figure 3. Wave height parameter for the 0.5 m drop height category in the three bed lengths

The maximum wave height during propagation is obtained at the instant when the wave starts to reflect from the downstream dam which acts as the obstruction. This wave reflection dampens the remaining waves with the aid of viscous effects. Figure 3 shows the wave height parameter variation after the wave reflects by hitting the downstream dam.

Figure 4 shows the variation of free surface movement in terms of its velocity. The results obtained for the 0.5 m drop height model helps in predicting the behaviour of these waves in the subsequent models. In this case, where the drop height is low, it is evident that the potential energy will be lesser than the other two cases. Also the result of this potential energy change to kinetic energy of the wave motion is predictable through the variation in wave amplitudes. It was also verified that the reservoir had sufficient depth to dampen the waves, hence in this type of problem, unless the reservoir catchment is low, the shallow water wave theory and the shallow water equations (SWE) does not hold good.

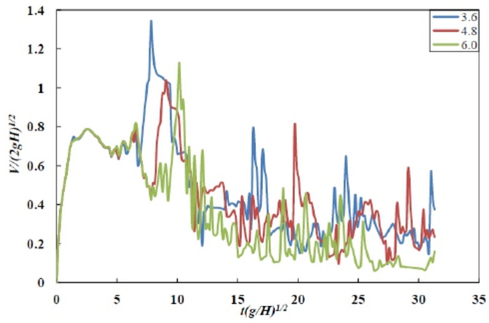

Figure 4 Velocity parameter for the 0.5 m drop height category in the three bed lengths

In the 1.0 m drop height category, the maximum wave height parameter (*h/H*) developed is 1.2677, see Figure 5. Also the maximum wave height in these 3 models immediately after the impulse was observed at about the time parameter value 2.98. In these three models, the location of maximum wave height immediately after the impulse was observed at about 2.61 m from the leftmost wall. Despite the increase in potential energy of the dam break model in the 1.0 m drop height category, the maximum wave heights observed near the downstream dam wall are almost similar to the 0.5 m category. This may be considered due to the higher relative depth in the reservoir where the wave propagates.

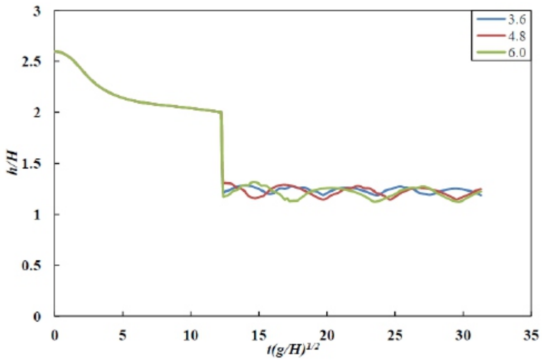

Figure 5. Wave height parameter for the 1.0 m drop height category in the three bed lengths

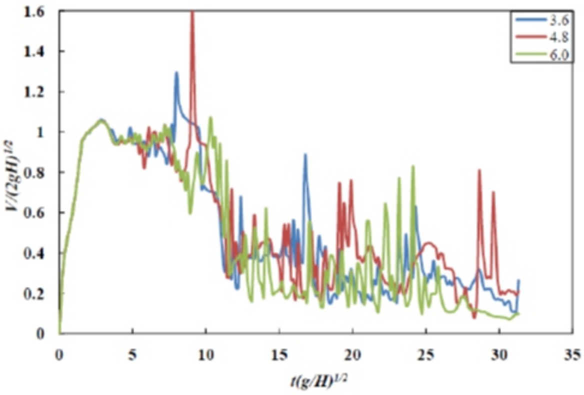

Figure 6. Velocity parameter for the 1.0 m drop height category in the three bed lengths

The wave rise as the impulse is generated increased in the 1.0 m drop height category even though near the obstruction, the wave heights remained nearly the same. Figure 6 shows the variation of wave velocity for the three models having 1.0 m drop height. The run up occurs faster, but the maximum level rise is almost identical to the 0.5 m category. This can be attributed to the high turbulence that occurs with the formation of a larger air pocket inside the impulse wave volume. It is evident from the variation of wave velocity parameter plot (Figure 6) that there is higher mass transport in the shorter bed length model and the viscous effects in reducing the wave characteristics is lower compared to the other two cases. The low amplitude liquid vibrations are higher in the longer bed length models and high amplitude in short bed length model.

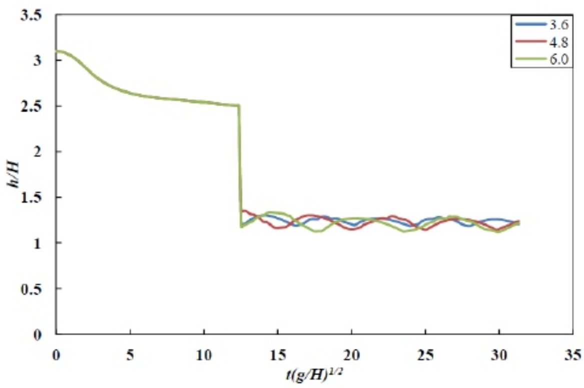

Figure 7. Wave height parameter for the 1.5 m drop height category in the three bed lengths

In the 1.5 m drop height category, the maximum wave height parameter (*h/H)* developed is 1.286, see Figure 7. Also the maximum wave height in these three models immediately after the impulse was observed at about the time parameter value of 3.13. In these three models, the location of maximum wave height immediately after the impulse was observed at about 2.66 m from the leftmost wall. It may be noted that there is a significant rise in the water levels as the potential energy of the dam break model increases.

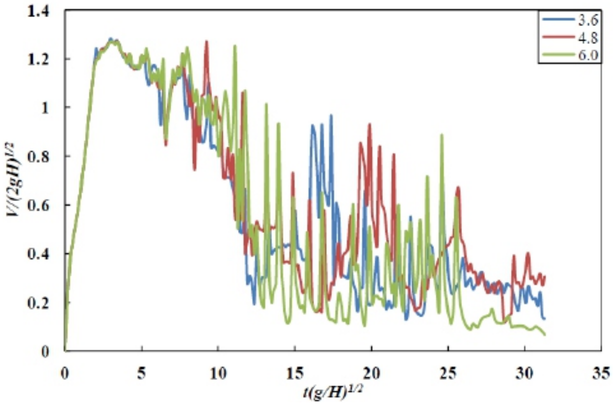

Figure 8. Velocity parameter for the 1.5 m drop height category in the three bed lengths

Figure 8 shows the wave velocity parameter for the 1.5 m drop height category of models. From the wave amplitude plots for all the three categories, it was observed that the two longer bed length models produced almost identical wave heights towards the end of the simulation time as the wave dampens. In all the three cases the shorter model produced higher amplitudes and more cycles of vibration.

Table 2 shows the maximum wave rise near or at the downstream dam wall in all models. There are approximately 5 to 8 times rise in water levels for the 1.5 m drop height category compared to 1m category except for the shorter bed length case. There is no significant rise in water levels when 1 m drop height models and 0.5 m models are compared.

Table 2 Wave rise observed near or at the downstream dam wall in all flatbed models

Drop height (m)	Bed length (m)	Time parameter	Wave height ratio
0.5	3.6	5.64	1.37
	4.8	6.89	1.35
	6	8.14	1.335
1	3.6	5.79	1.37
	4.8	7.05	1.352
	6	8.3	1.339
1.5	3.6	5.95	1.387
	4.8	7.2	1.366
	6	8.46	1.355

6. Conclusions

Free surface flow of an advancing wave front due to a dam break was simulated. The problem resembles either a steady flow in an open channel or a dam breaking into the tailrace generating impulse waves. Numerical investigations were conducted on nine different models having variations in bed length and drop height or fall height of the dam break. The characteristics of the generated wave were observed for the type, transformation and suppression. It was observed that as the drop height increases the time taken to reach the maximum wave height also increases. This also shows increasing rate with the increase in the bed length of downstream reservoir within each drop height.

High energy transport occurs in the third drop height category as the wave height ratio indicates. Only the longest bed length model simulated a lesser height ratio compared to the other two category, that too only when compared to the shorter ones. The relative wave height increase for the third drop height category is nearly 8 times larger than that of the other two categories.

References

- *Abdolmaleki, K., Thiagarajan, K.P., Morris-Thomas, M.T., 2004. Simulation of the dam break problem and impact flows using a Navier-Stokes solver, 15th Australasian Fluid Mechanics Conference. Sydney, Australia.*
- *Chang, T.J., Kao, H.M., Chang, K.H., Hsu, M.H., 2011. Numerical simulation of shallow water dam break flows in open channels using smoothed particle hydrodynamics. Journal of Hydrology, Vol.408, 78-90.*
- *Colagrossi, A., Landrini, M., 2003. Numerical simulation of interfacial flows by smoothed particle hydrodynamics. Journal of Comp. Phys., Vol. 191, No. 2, 448–475.*
- *Donea, J., Giuliani, S., Halleux, J.P., 1982. An Arbitrary Lagrangian–Eulerian finite element method for transient dynamic fluid structure interactions, Comput. Methods Appl. Mech. Engrg., Vol. 33, No. 1, 689−723.*
- *Gopalakrishnan, T.C., Tung, C.C., 1980. Run-up of steep breaking waves – a finite element approach. Journal of Coastal Engrg, Vol. 4, No. 1, 3–22 .*
- *Heller,V., Hager, W.H., Minor, H.E,.2009. Landslide generated impulse waves in reservoirs – basics and computation. Technical Report, VersuchsanstaltfürWasserbau, Hydrologie und Glaciologie, Zurich.*
- *Hirt, C.W., Nichols, B.D.,1981. Volume of Fluid (VOF) method for the dynamics of free boundaries. Journal of Comp. Phys., Vol. 39, No. 1, 201–225.*
- *Huerta, A., Liu, W.K., 1988. Viscous flow with large free surface motion, Comput. Methods Appl. Mech. Engrg., Vol. 69, No. 3, 277−324.*
- *Litrico, X., Fromion, V., 2009. Modeling and Control of Hydrosystems. Springer, London, UK.*
- *Scardovelli, R., Zaleski, S.,1999. Direct numerical simulation of free-surface and interfacial flow. Journal of Annu. Rev. Fluid Mech. Vol. 31, No. 1, 567–603.*
- *Shin, S., Lee, W.I., 2000. Finite element analysis of incompressible viscous flow with moving free surface by selective volume of fluid method. International Journal of Heat & Fluid Flow, Vol. 21, No. 2, 197−206.*
- *Stoker, J.J., 1957. Water Waves: The Mathematical Theory with Applications, Pure and Applied Mathematics. Interscience publishers, Inc., New York.*
- *Wood, D.J., Pedersen, G.K., Jensen, A., 2001. Modelling of run-up of steep non-breaking waves by FLUENT, Mechanics and Applied Mathematics. Oslo, Norway.*
- *Wood, D.J., Pedersen, G.K., Jensen, A., 2003. Modelling of run-up of steep non-breaking waves. Journal of Ocean Eng., Vol. 30, No. 5, 625–644.*
- *Yeh, H.H, Ghazali, A., Marton, I.,1989. Experimental study of bore run-up. Journal of Fluid Mechanics, Vol. 206, 563-578.*
- *Yue, B.,Wang, Z., 2006. Numerical study of three-dimensional free surface dynamics. ActaMechSinica, Vol.*

Ventilation Systems and Its Implication on IAQ and Energy Efficiency in Buildings

Shailza Singh *
CBRI,Roorkee,247667,India

A B S T R A C T

This article gives a brief review of the ventilation systems employed in buildings, the air flow rates and its dependence on Indoor Air Quality (IAQ) . The aim is to provide some insight to architects, building engineers and contractors who play an important part in selecting the ventilation systems.

A R T I C L E I N F O
Article history:
Received 01 July 2016
Accepted 19 August 2016

Keywords : Ventilation strategies; Air flow rates; IAQ

1. INTRODUCTION

Building ventilation has a huge implication on the overall indoor environmental quality, particularly, thermal comfort, indoor air quality (IAQ) and its energy-use pattern. Too little ventilation may result in poor indoor air quality, while too much may cause unnecessarily higher heating and cooling loads. Recent advances in building ventilation (Nielsen, 1993; Etheridge and Sandberg, 1996; Skistad et. al., 2004; Awbi, 2011; Müller et. al., 2013) have refined the ventilation rates with efficient energy-use but many studies have evidently raise the issue of poor IAQ in the past few years (Fisk, 2000, Fanger, 2006; Boestra and van Dijken, 2010). The need of building occupants for optimum ventilation rates has been invigorated by researchers to not only provide comfort and good air quality (European Collaborative Action, 1992) but also to optimize the energy consumed on achieving the indoor environmental quality.

In India, buildings are responsible for 35% of total energy consumption with an annual rise of 8% (Manu, S., et.al. ,2016). Reports show that the cooling load accounts for up to 45% of the total electricity consumption in residential sector (BEE,2007) and 31 % in commercial buildings ((Manu, S., et.al. ,2016).). An average HVAC (Heating, Ventilation and Air Conditioning) load per unit area lies within the range of 120-290kWh/m^2/year for conditioned buildings in India (P.A.C.E- D. , 2014). This high dependence on HVAC systems and high expectations of comfort levels demands the assessment of current methods of building ventilation and developing ventilation strategies with improved IAQ and energy performance. A wide range of ventilation system is available to meet the satisfactory environmental conditions each having the potential to meet specific application. But, the decisions on whether to provide natural, mechanical (i.e. supply-only, exhaust-only, or both supply and exhaust) or hybrid ventilation depends on several factors. Local climate, building type, building configuration, IAQ, cost, heating/cooling load and occupant's behavior primarily dictate the type of ventilation strategy to be adopted. Considering the highly variable climate of India, there is a need for assessing different ventilation strategies so as to develop guidelines that are capable of providing better indoor spaces with improved thermal environment. In India, we don't have any set of standards on ventilation that focus on IAQ and energy-use. National building Code, has recommended values of air flow rates for different types of buildings but this requires a thorough revision, considering the current exposures to the health risk of indoor pollution in buildings.

This article gives a brief review of the ventilation systems employed in buildings, air flow rates and its dependence on IAQ dependence of IAQ. The aim is to provide some insight to architects, building engineers and contractors who play an important part in selecting the ventilation systems. This will also help the research community in this area to develop new ventilation strategy with desired performance.

2. Ventilation systems: Natural Mechanical & Hybrid

Ventilation moves outdoor air, distributes it within the building or room and finally helps in diluting the pollutants originating in the building and removing the pollutants from it (Etheridge & Sandberg, 1996; Awbi, 2003). Good ventilation facilitates the comfort and safety of building occupants and is mostly subjected to a legal minimum requirement. Ventilation rate, Airflow direction and Air distribution or air flow pattern are the three basic elements of building ventilation. Natural, mechanical and hybrid ventilation are three broad categories of ventilation systems in any building.

2.1. Natural Ventilation

Building permeability and ventilation opening plays a key role in natural ventilation. A well designed naturally ventilated strategy combines the benefits of permanently open vents to provide background ventilation and controllable openings to meet the transient demand. To ensure that the ventilation is confined to air flow through the provided openings only, it is important that the building structure is tight. This helps in enhancing the ventilation performance by preventing air infiltration. The airflow within enclosed space is governed by the pressure differences due to wind and buoyancy forces. It is, therefore, important to have a thorough understanding of the pressure distributions in and around the building to design a building with efficient naturally ventilated system. Wind is the main cause of natural ventilation but in the absence of wind, the alternative is to implement stack pressure which can be created naturally by density differences to drive a ventilation flow through the building. Tall solar chimneys, light wells or atria are few of the architectural features that can be employed to enhance the stack effect. A lot of work has been going on in perfecting the natural ventilation strategy but still the prediction and control of indoor environment remains an open issue. Most of the researches are inclined towards the fluid mechanics of natural ventilation , physics of thermal stratified flows, prediction of pressure coefficients on building facades, behavioral aspects of window opening by occupants and current barriers or difficulties faced by natural ventilation in gaining regulatory acceptance. But, the effect of interior heat gains on the flow rates due to buoyancy forces developed as a result of temperature difference has shifted the focus of many researchers in past few years. Few researchers have also worked on assessment of passive strategies for cooling and ventilation with a prime focus on the heat model coupling, external and internal thermal mass (Zhou et.al.), use of night time cooling in moderate climates (Wang et.al.), efficiency of wind catchers or wind towers.

Natural ventilation has its limitations also as, sometimes; inadequate control over air flow rates can adversely affect the indoor air quality. It was noted that the uncertainties associated with the driving forces is due to different principles of natural ventilation i.e. single sided ventilation, cross ventilation or stack effect [Chenari B., et.al]. The effectiveness of natural ventilation depends upon the outdoor environmental conditions. For e.g. outside wind speed of 3.0m/s is required to cool down the indoors using natural ventilation (Ohba. M. and Lun. I.,2010) or it is unsuitable to open windows when outdoor air is hot or polluted. It is not suitable for extreme hot or cold conditions It is important that minimum ventilation rate required for better IAQ and maximum ventilation for summer cooling is thoroughly evaluated.

2.2. Mechanical ventilation

Mechanical ventilation (MV) is based on the distribution of the pre-conditioned air (heated/cooled) to an enclosed space through ducts and delivered by air-diffusion outlets. It provides uniform ventilation rates as compared to natural ventilation and can respond to the varying needs of occupants to and, if designed properly. One major advantage of mechanical system over natural ventilation is that it provides great flexibility for controlling the indoor environment. The air distribution is the key element in mechanical ventilation systems to condition the spaces and to achieve acceptable indoor thermal conditions (Balaras, C.A.). Mixing ventilation (MV) and Displacement ventilation (DV) are the two widely used air distribution systems. Mixing ventilation works on the principle of mixing the incoming fresh air, supplied at a high velocity (typically> 2.0 m/s) through the ceilings or upper part of the walls, with the indoor air (Cao. G. et.al., 2014). It uniformly distributes the thermal energy of the enclosed air and dilutes the contaminant concentration of the room. Although, it is well documented in various ventilation guides and standards (e.g., ASHRAE Handbook, 2011), it is known to be inefficient in terms of providing good indoor air quality and energy performance.

In displacement ventilation cool air is introduced at a low velocity (typically <0.5m/s) at or near the floor to create an upward air movement or thermal plumes (Cao. G. et.al., 2014). As the room air movement is primarily driven by buoyancy forces, creating vertical gradients of air temperature and contaminant concentration, this method can only be used for cooling. However, it requires lower fan power and has higher ventilation effectiveness than mixing ventilation and, therefore, provides an energy efficient method of air supply in buildings. As the calculation of airflow in the plume above the heat source is too complex and time consuming and , thus, requires software based approach i.e. Displacement Ventilation Software and/or computational fluid dynamics based software packages to design. Though displacement ventilation systems are successfully used in the Northern Europe and some parts of USA, its exposure to warmer climates still remains limited (Livchak,A., Nall. D., 2001) and requires a much needed research.

2.3. Hybrid ventilation

Hybrid ventilation, as defined in International Energy Agency (IEA) Annex 35 (1999), is a two-mode system that provides necessary indoor air quality in an energy efficient way by switching automatically from one mode to another (i.e. from naturally ventilated to mechanical or vice versa) in different time of the day, season or a year. Studies show that natural ventilation unable to maintain the IAQ and thermal comfort in acceptable levels. Therefore, an integrated approach with passive cooling and passive solar heating is combined with the mechanical system to optimize the overall energy-usage of the building. This approach is characterized by the use of windows and doors for space ventilation and HVAC systems only when the wind pressure and temperature gradients are not sufficient to drive the flow by natural means (Heiselberg, P. et.al. ,2001 and Van Heemst, L.V. (2001). Overall, hybrid ventilation is a low-energy alternative to energy-intensive air-conditioned buildings or naturally ventilated buildings with poor occupancy comfort and control levels (Turner, W.J.N. and Awbi, H.B. (2015).

A project named HybVent by IEA initiated the state of the art work on hybrid ventilation solutions in contemporary buildings. Twenty two buildings (seven renovated and fifteen new constructions) were analyzed for stack effect using dedicated ducting or through corridors/hallways and control strategies. Many researchers have highlighted the performance of hybrid ventilation in buildings (Turner, W.J.N. and Awbi, H.B. ,2015; Sherman, M.H., 1997; Brager, G.S., de Dear, R.,2000; Taylor, N.J., et.al.,2012) using numerical methods (Homod, R.Z. ; Sahari, K.S.M., 2013), computational modeling (Turner, W.J.N., Walker, I.S.,2013) and very few experimentally (Niachou, K., et.al., 2008; Yoshino. H., et.al.,2003). In a study by Schulze and Eicker, air flow rate for different openings indicated that indoor air quality is maintained at acceptable levels but thermal comfort varied when used with natural ventilation strategies. Another study investigated the effect of ventilation rates on IAQ and energy saving in a single-family house. It is inferred that the ventilation rate of 0.3ACH is sufficient to maintain IAQ at acceptable level with optimum energy-use as compare to the one proposed by Swedish Building Standards (i.e. 0.5ACH). Few of the researchers have also used tracer gas experiments to analyze the air flow rates of hybrid ventilation system (Niachou, K., et.al., 2008). Kim & Hwang assessed the hybrid ventilation system with natural supply inlet and mechanical exhaust in apartments in Korea using computational fluid dynamics. They inferred that this system has achieved the perceived IAQ but has also increased the space heating load.

Hybrid ventilation works on the principle of natural and mechanical ventilation, fan-assisted natural ventilation or stack and wind assisted mechanical ventilation. These principles when used in conjunction with the control strategies can improve the energy performance of hybrid ventilation system [Chenari B., et.al ,110]. The control strategy is framed by assigning set points for certain parameters i.e. indoor /outdoor temperatures, relative humidity, CO_2 concentrations, wind speed and wind direction. Hybrid ventilation systems generally comprises of an inlet, distribution unit, outlet, fan, and in some cases heat exchanger (Lim. Y et.al.,2015).Demand-controlled ventilation, based on the occupancy levels and concentration of pollutants, is also being studied by the researchers. It is suitable for spaces where the occupancy levels vary frequently such as lecture halls, theaters, shopping malls etc. Impinging jets (IJ) and Confluent jets (CJ) are the two new hybrid ventilation concepts that combine the characteristics of both MV and DV (Cao. G. et.al.,2014).

The feasibility of this ventilation system for Indian climatic conditions can resolve issues related to the energy load of a building and demand a thorough investigation via integrated research strategies (i.e. experimental/computational).

3. Ventilation Rates

Ventilation rates and outdoor air requirements of the building depends upon its architectural design, typology/ function and occupancy distribution (density per floor area), concentration of indoor/outdoor contaminant and climatic changes in the surrounding environment. Therefore, provisions to control the airflow rate to meet the current prevailing demand are desirable. (Energy-Efficient Ventilation for Apartment Buildings, Rebuild America program, LBNL)

Ventilation system has evolved manifolds, since the early 1970s, under the pioneering work of the researchers (European Collaborative Action, 1992, Awbi, 2003, 2007; Karimipanah et al., 2007, 2008,Cao. G. et.al.,2014) who demonstrated the importance of ventilation rates on comfort and health safety of the occupants. But, it was not until 1836 that the ventilation rates are quantified and were addressed to be regulated under standards (with recommended value of 30cfm/person or 14L/s per person). ASHRAE Standard 62-1973, Ventilation & Acceptable Indoor Air Quality, was the first of its kind during that period with minimum and recommended for kitchen and bath areas. It is important to note that the earliest history of ventilation rates is applicable to all the building types. In the next version i.e. Standard 62-1981, the ventilation rates are reduced in order to reduce the energy consumption (this was proposed immediately after the oil crisis hit the world in 1970's). In the 1989 version of Standard 62, the contribution of occupants and materials as a source of pollutants is recognized in low occupant density buildings. The basic drawback of the Standard 62-1989 is that it did not clarify as to how to achieve the minimum ventilation rates. Later, Standard 62.2 introduced the additivity approach for calculation of ventilation rates and building part is added to a people part such that the air change rate is a function of occupancy density. There have been a lot of revisions in ventilation rates since the first version of the standard. The ventilation rates depend primarily on the source of contaminants, its emission and impact on the occupants. The standard specifies that a minimum outside air change rate should be based either on the volume of the space to be ventilated or on the number of occupants. It allows a minimum of 0.35 air changes per hour (ACH) per cubic foot of ventilated space, or 15 cubic feet per minute (CFM) per person, whichever of the two is higher for apartment buildings (Energy-Efficient Ventilation for Apartment Buildings, Rebuild America program, LBNL)

4. IAQ and ventilation rates

IAQ is, basically, a descriptor of the amount and type of contaminants in the air. (Chenari B., et.al., 2016). Environmental Protection Agency (EPA) has listed Indoor Air Quality as one of the top five environmental Health Risks, as people spends 80% of their time indoors. There is a, therefore, a strong drive to design effective ventilated strategies with optimum energy costs (Livchak. A., Nall. D., (2001). In the past few decades, indoor environmental quality standards have become more stringent as the expectation level of occupants and heating/cooling loads of the buildings have increased (Balaras. C.A.).

ASHRAE has defined IAQ as the acceptable indoor air in which the concentration of pollutants is not at identified harmful level and the occupants (80% or more) do not express dissatisfaction. In the beginning, up to 20th century, occupants were considered to be the main source of indoor pollution like human bio-effluents and/or tobacco smoke. Indoor Air Quality (IAQ) is achieved through proper ventilation by replacing stale indoor air by fresh outdoor air. The air flow rates helps in achieving the required dilution and mostly determined by the pollutant's generation rates. As discussed earlier, the process can be natural, mechanical or a combination of both the strategies. The ventilation rates are established either by adding the necessary flow rates to dilute the pollutant or by choosing the maximum ventilation rates. But in majority, the ventilation rates are determined on the basis of the comfort criteria of 20% PPD of people whose sensory perception has not adapted to that environment. (Chenari B., et.al., 2016).

Indoor Air quality is a function of temperature, air-flow, window position (window to wall ratio) and CO_2 concentrations (Menassa, C.C., et.al. (2013). Ventilation standards/ guidelines were framed on the basis of metabolic CO_2 concentration. But with the advancements in the field of ventilation strategies and pressing need of meeting the health standards in buildings, ventilation guidelines now takes into account both occupant generated contaminants (e.g. odors, CO_2) and non-occupant sources (e.g. VOCs from building materials and furnishing) (Charles,K. et.al. (2005). CO_2 is not necessarily a contaminant up to a certain level (threshold CO_2 level above 1000 ppm is considered dangerous) and, therefore, is used as a tracer to ensure the ventilation performance of the buildings. The most efficient strategy to maintain indoor air quality is to remove the contaminants at the source and then rely on ventilation (dilution) to remove the air-borne VOCs (Charles,K. et.al. (2005).

5. Conclusion

Earlier, mechanical ventilation appeared to be a practical solution to natural ventilation for year-round control of indoor environmental conditions. And this subsequently has resulted in the replacement of natural ventilation in most of the buildings (especially commercial complexes). Studies have shown that natural and mechanical ventilation systems can, in practice, be equally effective for maintaining the indoor environmental quality and energy efficiency. However, natural ventilation only works when the local driving force is available (for example, winds or breezes). On the other hand, mechanical ventilation has certain limitations, involved in properly installing and maintaining, that may lead to a high concentration of indoor pollutants and ultimately result in a low indoor air quality with higher health risks. Hybrid ventilation does looks promising, in terms of IAQ and energy efficiency, but requires a case-specific approach and a detailed structure of ventilation design. It is important to understand that the ventilation guidelines are mostly expressed in terms of air flow rates and there is no mention of IAQ so far. With the current trend of rise in outdoor and indoor pollutant level, it is high time that we revive and reform our ventilation strategies in India, considering the building type, occupancy level and climatic zone. And, finally, to achieve energy efficient ventilation system with improved IAQ it is important that the government, businesses and individuals transform the way the buildings are designed, built and operated.

REFERENCES

- *Awbi, H. B. (2011). "Energy efficient ventilation for retrofit buildings," in Proceedings of 48th AiCARR International Conference Energy Performance of Existing Buildings (Baveno), 23–46.*
- *Balaras, C.A. Air Conditioning- Energy Consumption and Environmental Qulaity- Mechanical Ventilation and Equipment. National Observatory of Athens, Hellas, Greece.*
- *BEE. Energy Conservation Building Code 2007. Bureau of Energy Efficiency*
- *Boestra, A., and van Dijken, F. (2010). Indoor environment and energy efficiency of schools. REHVA J. 47, 33–38.*
- *Brager, G.S., de Dear, R. (2000). A standard for natural ventilation, ASHRAE Journal,42(10), 21-29.*
- *Cao. G. et.al. (2014). Review of performance of different ventilation and airflow distribution systems in buildings. Building and Environment, 73, 171-186.*
- *Charles,K. et.al. (2005). Indoor Air Quality Guidelines and Standards, National Research Council, Canada.*
- *Chenari ,B., et.al. (2016). Towards sustainable, energy-efficient and healthy ventilation strategies in buildings: A review. Renewable and Sustainable Energy Reviews. 59, 1426-1447).*
- *Energy-Efficient Ventilation for Apartment Buildings, Rebuild America program, Lawrence Berkeley National Laboratory (LBNL).*
- *Etheridge, D., and Sandberg, M. (1996). Building Ventilation: Theory and Measurement. Chichester: Wiley.*
- *European Collaborative Action. (1992). Guidelines for Ventilation Requirements in Buildings. Report No. 11, EUR 14449EN. Luxembourg: Commission of the European Communities.*
- *Fanger, P. O. (2006). What is IAQ? Indoor Air, 16, 328–334. doi:10.1111/j.1600-0668.2006.00437.x*
- *Fisk, W. J. (2000). Health and productivity gains from better indoor environment and their relationship with building energy efficiency.Annu. Rev. Energy Environ. 25, 537–566. doi:10.1146/annurev.energy.25.1.537*
- *Heiselberg, P. et.al. (2001) Hybrid Ventilation: State of the Art Review, IEA. Annex 35 Hybrid Vent. New Retrofit. Off.Build. http://hybvent.civil.auc.dk/puplications/stateoftheart_text.htm*

- *Homod, R.Z. ;Sahari, K.S.M. (2013). Energy savings by smart utilization of mechanical and natural ventilation for hybrid residential buildings model in passive climate. Energy and Building. 60,310-329.*
- *Karimipanah, T., et.al. (2007). Investigation of air quality, comfort parameters and effectiveness for two floor-level air supply systems in classrooms. Build. Environ. 42, 647–655. doi:10.1016/j.buildenv.2005.10.016*
- *Karimipanah, T., et.al. (2008). The air distribution index as an indicator for energy consumption and performance of ventilation systems. J. Hum. Environ. Syst. 11, 77–84. doi:10.1618/jhes.11.77*
- *Lim. Y et.al. (2015). Indoor Environment Control and Energy Saving Performance of ˆG Hybrid Ventilation System for a Multi-residential Building. Energy Procedia, 78, 2863-2868.*
- *Livchak,A., Nall. D., (2001). Displacement Ventilation- Application for Hot and Humid Climate; Clima 2000/Napoli 2001 World Congress- Napoli(I), 15-18 .*
- *Manu, S., et.al. (2016). Field studies of thermal comfort across multiple climate zones for the subcontinent: India Model for Adaptive Comfort (IMAC). Building and Environment. 98, 55-70.*
- *Menassa, C.C., et.al. (2013). Optimizing hybrid ventilation in public spaces of complex buildings- A case study of the Wisconsin Institutes for Discovery. Building and Environment. 61, 57-68.*
- *Müller, D., Kandzia, C., Kosonen, R., Melikov, A. K., and Nielsen, P. V. (2013). Mixing Ventilation: Guide on Mixing Air Distribution Design. Brussels: REHVA Guidebook 19.*
- *Niachou, K., et.al. (2008). Experimental performance investigation of naural, mechanical and hybrid ventilation in urban environment. Building and ENvironemnt. 43,1373-1382.*
- *Nielsen, P. V. (1993). Displacement Ventilation: Theory and Design. Denmark: Aalborg University.*
- *Ohba. M., Lun. I.(2010). Overview of natural cross ventilation studies and the latest simulation design tools used in building ventilation-related research. Advances in Building Energy Research,4, 127-166.*
- *P.A.C.E.-D. Technical Assistance Program, HVAC Market Assessment and Transformation Approach for India, New Delhi, 2014, http://www.pace-d.com/wp-content/uploads/2014/08/HVAC-Report-Send-for-Printing-Low-Res.pdf.*
- *Sherman,M.H., (1997). Residential ventilation and energy characteristics, LBNL-39036, ASHRAE Trans.103,27.*
- *Skistad, H., Mundt, E., Nielsen, P. V., Hagström, K., and Railio, J. (2004). Displacement Ventilation in Non-Industrial Premises. Brussels: REHVA Guidebook 1.*
- *Taylor, N.J., et.al. (2012). An experimental approach to optimizing natural ventilation in public spaces of complex buildings. Construction REearch Congress Conference, Purdue University.*
- *Turner, W.J.N. and Awbi, H.B. (2015). Experimental investigation into the thermal performance of a residential hybrid ventilation system. Applied Thermal Engineering, 77, 142-152.*
- *Turner, W.J.N., Walker, I.S. (2013). Using a ventilation controller to optimize residential passive ventilation for energy and indoor air quality. Building and Environment. 70,20-30.*
- *Van Heemst, L.V. (2001). Hybrid Ventilation : AN integral solution for ventilation , Health and Energy, TU-Delft , Delft ,The Netherlands. http://hybvent.civil.auc.dk/puplications/paper%20met%20kaft-scherm.pdf*
- *Yoshino. H., et.al. (2003). Performance analaysis on hybrid ventilation system for residential buildings using a test house. Indoor Air. 13, 28-34.*

Apparent shear stress in an asymmetric compound channel

Kamalini Devi[1], Kishanjit Kumar Khatua[2], Subhalaxmi Sial[3]

[1 & 3]Research Scholar,Department of Civil Engineering,National Institute of Technology Rourkela,769008 India.

[2] Associate Professor,Department of Civil Engineering,National Institute of Technology Rourkela,769008 India.

[1]Email:kamalinidevi1@gmail.com ,2Email:kkkhatua@nitrkl.ac.in ,3Email:subhalaxmisial@gmail.com

Mobile No.:1+91 8763866 544, 2+91 9861068 249, 3+91 9439751 814

A B S T R A C T

In a compound channel section, there is always transfer of momentum between the deep main section and the adjoining shallow floodplains. Channels are often flanked by one flood plain either side of it, known as asymmetrical compound channels. So occurrence of the strong turbulence at the junction between main channel and flood plain results the transport of the longitudinal momentum and the vertical plain between the main channel and flood plain will experience an appreciable longitudinal turbulent shear stress in the flow direction which referred to as apparent shear stress. Momentum transfer phenomenon has the effect of increasing floodplain shear and decreasing main channel shear. In a symmetrical compound channel the momentum transfer occurs from both sides of the channel to the flood plains uniformly. But in case of a compound channel with asymmetrical floodplain, there is a stronger interaction between main channel and flood plain occur as compared to the symmetrical case causing the boundary shear stress distribution more non-uniform as compared to the symmetrical cases. Experiments are carried out to measure the boundary shear stress around the wetted perimeter of a two-stage asymmetric compound channel that helps to quantify the momentum transfer in terms of apparent shear stress along the interfaces. Analysis of the apparent shear is useful in deciding the choice of appropriate interface plains for developing stage-discharge relationship of a compound channel. In the present work, a modified expression to predict the apparent shear stress in an asymmetrical compound channel is developed. From the error analysis, the developed model is found to predict the apparent shear stress better than models of other investigators.

Keywords:*Apparent shear, boundary shear stress distribution, interface plane, asymmetrical channel, floodplain, main channel, overbank flow, momentum transfer.*

1. INTRODUCTION

At the time of flood, a part of flow is carried out by river main channel and the rest discharge is carried out by its adjoining one or both side flood plain. The channel is known as symmetric compound channel when both flood plains are equal otherwise the river channel is referred to as asymmetric compound channel, where it has one sided flood plain. Once the channel appears as a compound section, the flow structure undergoes a steep change for such section. This flow structure is characterized by the generation of large shear layer due to the significant difference of velocity between the main channel and flood plain. The transfer mechanism of momentum in a compound channel was first investigated by Sellin(1964). Zheleznyakov(1965) indicated the presence of artificial boundary made up vortices acting as a medium of momentum transfer between the main channel and flood plain at the junction.It has been observed that there is non-uniformity in the boundary shear distribution along the wetted perimeter of the section due to this momentum transfer (e.g., Ghosh and Jena 1971, Rajaratnam and Ahmadi 1979, Knight and Hamed 1984, Patra &Khasstua 2006). At shallow depth of flow over flood plain, momentum transfers from main channel to flood plain leading to the decrease in the main channel velocity and flow, while for reverse case, the transfer of momentum occurs from flood plain to main channel. Due to this interchange of momentum, the difference in boundary shear stress distribution occurs (e.g., Ghosh and Jena 1971, Rajaratnam and Ahmadi 1979.

Regarding the characteristics of boundary shear distribution, it has been stated that it helps to understand the resistance relationship, check the stability of bed material, design of stable channels and construction of retaining wall. Distribution of this parameter mainly depends on the shape of the cross sectional geometry and secondary flow structures.This secondary flow leads to the variation of local shear stress distribution from point to point in the wetted perimeter of the cross section due to the dissimilar subsection flows and also increases the flood plain shear by decreasing the main channel shear.(e.g., Rajaratnam and Ahmadi 1979, Myers 1977, W.R.C. &Elsawy1975).So proper distributions of boundary shear stress in main channel and flood plain needs to be found out so that it will help to predict the stage discharge relationship for compound channel.

There are many traditional methods are being used for calculating the flow capacity for compound channel. They are Single Channel Method (SCM) and Divided Channel Method (DCM). The SCM usually under estimate the flow as it takes the whole compound section as one unit. The DCM over estimates the flow and makes the total compound section into some homogenous subsections by introducing three imaginary interfaces (vertical, horizontal and inclined interface) at the junction region. This approach finds average flow velocity for each compartment therefore predicts better overall discharge primarily by the hydraulic engineer (Weber and Menéndez 2004, and Patra and Khatua 2006).Many researchers have proved the adequacy of proper selection of imaginary interface for accurate estimation of stage discharge relationship (e.g., Ackers 1992, Wright and Carstens 1970, Wormleatonet al. 1982, Patra and Khatua 2006 and Huttof et al. 2008) etc. Most of the approaches are suitable for symmetrical compound channel and found to give poor result for asymmetrical compound channel. DCM is popular and is being still used in many software applications. The choice of DCM depends upon the knowledge of apparent shear stress. Considering the above facts, an attempt has been made to analyse and develop an advanced model to predict the apparent shear stress in an asymmetrical compound channel.

2. Experimental details

For carrying out research, the asymmetrical compound channel is constructed using plain cement concrete inside rectangular steel tilting flume in the hydraulic engineering laboratory of the Civil Engineering Department, National Institute of Technology, Rourkela, India. This channel is having one flood plain at right side of it making the total width of the compound section 198cm (Figure1). The main channel is trapezoidal in cross section with 1:1 side slope having 33cm bottom width and 11cm at bank full depth. The longitudinal bed slope is taken as 0.001325. The roughness of the flood plain and main channel are kept same and estimated to be 0.01. The second series of data chosen for the present analysis are from a large scale compound channel facility i.e. the UK Flood Channel Facility, located at the laboratories of HR Wallingford Ltd shown in Figure (1). A Single set of available data from FCFfor asymmetrical compound channel of width ratio (α=2.7) is taken in to consideration. The geometrical parameters such as total width of main channel is 10 m, aspect ratio of main channel is 10, longitudinal slope of the channel is 0.001027 and Manning's roughness coefficient is 0.01. Finally the last series of data chosen for the present analysis are from the asymmetrical compound channel data of Al-Khatibet al. (2013). One series of the asymmetrical experimental data (width ratio 3) is considered from this which is conducted on the flume at the fluid mechanics laboratory, Mechanical Engineering Department, Birze it University. This asymmetrical glass-walled horizontal laboratory flume is 7.5m long, 0.30 m wide and0.30 m deep with a bottom slope of 0.0025. The manning's *n* is assumed as 0.015.

All the experiments in channel were also done under subcritical flow conditions. Plan view and sectional view of the NITR channel has been shown in Figure.1 and Figure.2. Boundary shear measurements on bed and wall as the shear stress was measured indirectly by Preston tube method using Patel's (Patel,1965) calibration curve. This is considered the best practice of measurement of boundary shear stress. Error adjustments to the shear value are done by comparing the corresponding shear values obtained from the energy gradient approach. The results so obtained by the two methods are found to be consistently within ±3% values

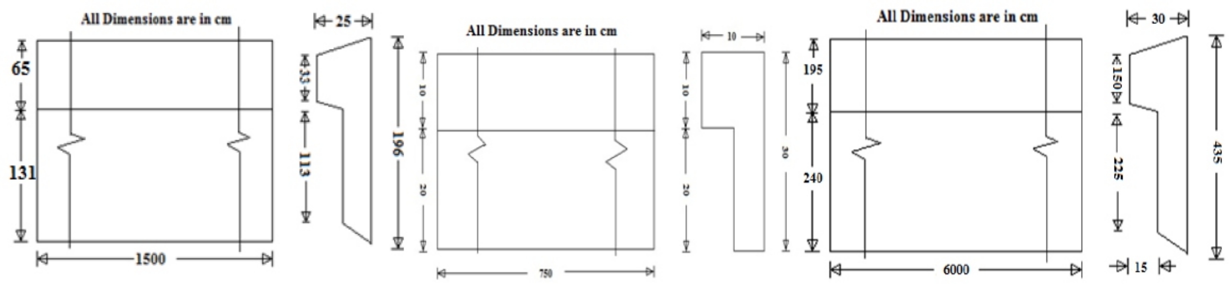

Figure 1 Plan and sectional view of experimental asymmetrical compound channels of NITR, Khatibet al. (2013) and FCF Series 6.

3. Analysis of results

3.1 Shear force results

The lateral exchange of momentum at the junction magnificently affects the shear stress distribution on each subsection. The boundary shear force resulted from the experiment on each subsection of the wetted perimeter were numerically integrated to give the mean boundary stress and the mean shear force. From the boundary shear force distribution, a brief idea regarding the transfer of momentum to different interfaces can be acquired. As the channel is of asymmetric flood plain, the values from either side are not equal due to the strong interaction at the junction. The wetted perimeter of the compound channel is divided into four parts i.e., the flood plain side slope, the flood plain bed, the main channel side slope and main channel bed. .

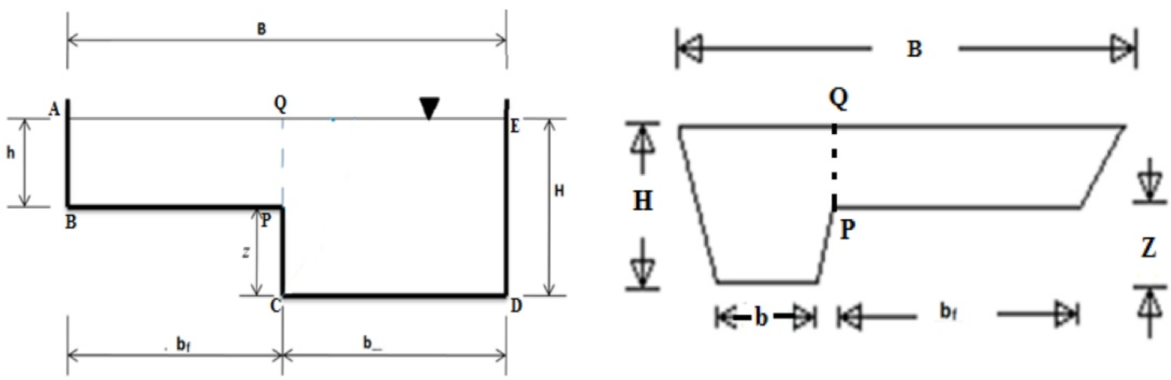

Figure 2 Sectional view of experimental asymmetrical rectangular and trapezoidal compound channels with vertical interface at junction

The boundary shear distributions for the FCF channel have been plotted in the Figure (3). The boundary shear stress measurements along the wetted perimeter of a compound channel for different flow depths and for different geometry are tedious. Further there are very limited data sets available regarding the boundary shear stress distributions in asymmetric compound channels. As our prime aim is to develop a generalized mathematical model to predict the apparent shear stress in an asymmetric compound channel, which in turns depend upon the boundary shear stress distribution therefore an attempt has been taken to extract the boundary shear stress distribution by an alternate but reliable approach. Shiono and Knight(1989) have proposed a numerical method popularly named as SKM method for accurately predicting boundary shear distribution in a compound channel. The method is widely and trustily used worldwide in the form of software known as Conveyance Estimation System (CES,Wallingford, UK). The accuracy of the SKM numerical approach to predict the boundary shear distribution has also been tested and presented in Figure (3). The method has been found to evaluate the boundary shear distribution more accurately with mean average error less than 5%.

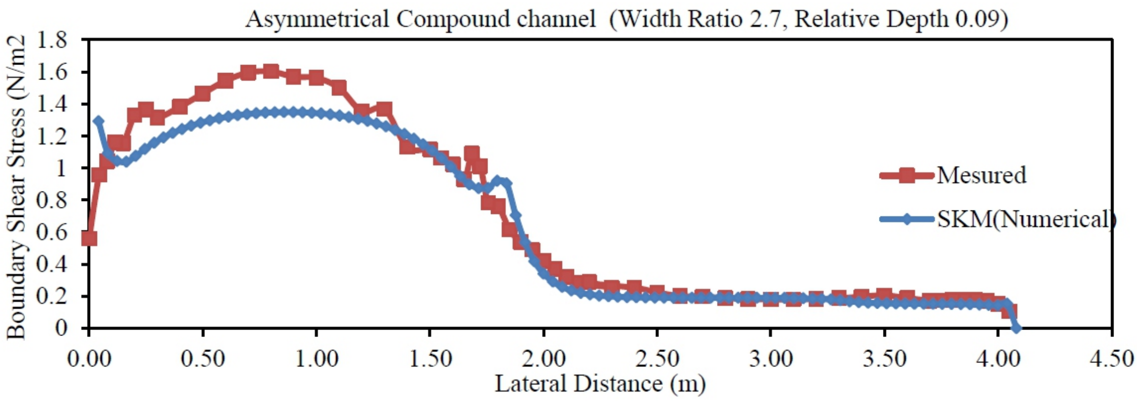

Figure3 Lateral distribution of the depth averaged boundary shear stress,tb for FCF Series 6.

As the present experimental in NIT asymmetric compound channel bears a single aspect ratio of 3 and width ratio of 5.1, the FCF channel bears single channel data sets with aspect ratio of 10 and width ratio of 2.7 and the experimental channel of Khatibet al.(2013) bears a aspect ratio of 5 with width ratio 3.0, so a wide range of data sets of various width ratio and aspect ratios have been generated using CES software. CES is based on Shion Knight Method (SKM)has been utilised to produce the boundary shear distribution for different channels having varying with ratio and relative flow depths. The principle of SKM is based on the simplification of continuity equation and Navier stokes equation given as

$$\rho\left[\frac{\partial \overline{UV}}{\partial y}+\frac{\partial \overline{UW}}{\partial z}\right]=\rho g S_0+\frac{\partial \overline{\tau_{yx}}}{\partial y}+\frac{\partial \overline{\tau_{zx}}}{\partial z} \qquad (1)$$

(i.e., secondary flows = weight force + lateral Reynolds stresses + vertical Reynolds stresses), where *x, y, z* = stream wise, lateral, and vertical directions, respectively; temporal mean velocity components corresponding to x, y z direction. τ_{yx} and τ_{zx} = Reynolds stress on plains perpendicular to the y and z directions respectively. ρ =water density; g= Acceleration due to gravity and S_0 = bed slope. Shiono and Knight (1989) obtained the depth-averaged velocity equation by integrating (1) over the water depth H and is simplified to

$$\rho\frac{\partial H(\overline{uv})_d}{\partial y} = \rho H g S_0 + \frac{\partial}{\partial y}\left(\rho\lambda H^2\left(\frac{f}{8}\right)^{\frac{1}{2}} U\frac{\partial U}{\partial y}\right) - \frac{f}{8}\rho U^2\sqrt{1+\frac{1}{s^2}} \qquad (2)$$

Where H the depth of flow $\overline{u}$ and $\overline{v}$ are the component of the mean velocity in x and y direction, $(\overline{u},\overline{v})_d$the product of the components and averaged over the flow depth, λ the eddy viscosity coefficient,f the local bed friction, sthe lateral slope and U the depth averaged velocity which is to be found out.

After the channel is divided into subareas in which the sub-area may be of constant depth domain or variable depth domain, the unknown constants can be solved by applying known boundaries like at junction and at rigid boundary. The boundary conditions applied for the present analysis are

1. $(U_d)_i = (U_d)_{i+1}$, due to continuity of depth averaged velocity
2. $\left(\frac{\partial U_d}{\partial y}\right)_i = \left(\frac{\partial U_d}{\partial y}\right)_{i+1}$, due to Continuity of the lateral gradient of the depth averaged velocity
3. $U_i = 0$No slip condition holds for the lateral position at the rigid side wall.

Applying these above boundary conditions for adjacent panels the equation (4) has been solved by a suitable MATLAB programming to find the depth average velocity form point to points laterally along the width of the channel and then the boundary shear has been found out from depth averaged velocity.The ranges of data sets produced belong to width ratio between 3 to 12 and depth ratio between 0.1 to 0.5. The ranges geometrical and flow parameters of the channels are tabulated in the table1.

Table 1 The geometrical and flow parameters of the channels considered for analysis

Series	Main Channel		Depth of flow (H)	Side Slope (s)	Bed Slope (S_0)	Relative Depth (β)	Aspect Ratio (δ)	Width Ratio (α)
	Bed Width(b)	Bank full Depth(z)						
Type1 (Trapezoidal)	1.5	0.15	0.167 0.1875 0.2142 0.25 0.3	1:1	0.001027	0.1 0.2 0.3 0.4 0.5	10	3,4 5,6 7,8 9,10 11,12
Type2 (Trapezoidal)	0.33	0.11	0.12 0.1375 0.157 0.18 0.22	1:1	0.00238	0.1 0.2 0.3 0.4 0.5	3	3,4 5,6 7,8 9,10 11,12
Type3 (Rectangular)	0.1	0.02	0.0222 0.028 0.0286 0.033 0.04	-	0.0025	0.1 0.2 0.3 0.4 0.5	5	3,4 5,6 7,8 9,10 11,12

3.2 Apparent shear stress on vertical interface

Considering the equilibrium of the main channel sub section of the asymmetrical compound channel (Figure 2), the total weight force along the main channel must be resisted by the sum of the boundary shear force acting on the channel wall and its bed and the apparent shear force at the interface. Let A_{mc} is the area of the main channel; τ_0 is the shear stress along the wetted perimeter; p the wetted perimeter of the compound channel; ρ density of water, g acceleration due to gravity, S_0 and longitudinal bottom slope of the channel and ASF_v is apparent shear force at the interface then we can write

$$\rho g A_{mc} S_0 = \int \tau_0 dP + ASF_v \quad 3(a)$$

$$ASF_v = \rho g A_{mc} S_0 - \int \tau_0 dP \quad 3(b)$$

To make the terms non dimensional, the Apparent Shear Force Ratio can be obtained by dividing the total driving force $\rho g A S_0$

$$ASFR_v = \frac{[\rho g A_{mc} S_0 - \int \tau_0 dP]}{\rho g A S_0} \quad (4)$$

Where A is the total cross sectional area of the compound channel. Knight and Demetriou (1983), Wormlenton (1984), Knight and Hammid (1984), Patra and Kar (2000), Khatua and Patra (2012), Mohanty and Khatua(2014) etc have shown that apparent shear force at the vertical interface depend upon the most influencing non dimensional parameter like width ratio (α), relative flow depth (β) and aspect ratio (δ). Looking to this point of view a step has been taken to find the dependency of apparent shear stress with these non dimensional parameters. Khatibet al. (2013) have presented experimental results on asymmetric compound channel with width ratio 1.5, 2 and 3 and developed a model to predict the discharge. FCF series-6 at Wallingford UK (http://www.birmingham.ac.uk) provides the detail experimental data of an asymmetrical compound channel with width ratio 2.7. Recently new experimentation on asymmetric compound channel with width ratio 5.1 has been done at hydraulics laboratory of NIT, Rourkela, India. We have used all the data sets for the present mathematical modelling and validation.

4. Results and discussions

Results of Apparent Shear Force Ratio ($ASFR$) in terms of single variable regression model have been presented and this data have been analysed to illustrate the effect of $ASFR$ on dimensionless parameters (α, β and δ) for several generated data sets in Figure 4 to 10. These data sets are having different width ratio and maintaining the same aspect ratio (δ) of their respective main channels (3 for NITR channel, 10 for FCF series and 5 for Khatibet al. 2013) as practiced in their respective experimental channels. Figure

4, Figure 6 and Figure 8 show the variation of apparent shear values (*ASFR)* with the flow depth for different width ratio (i.e., $\alpha = 3$ to 12).The functional relationship of *ASFR* with relative depth confirm a reduction of *ASFR* with increase of relative depth as shown in Figure 4, Figure 6 and Figure 8 for Type1, Type 2 and Type 3 channels. The graphs obtained from Figure 5, Figure 7 and Figure 9 indicates the *ASFR* decreases with increase in width ratio for Type1, Type 2 and Type 3 channels. Similar findings has also been observed by Prinos and Townsend (1984), Christodoulou and Myers (1999), and Moreta and Martin (2010).The dependency of *ASFR* with the flow depth and geometry has been tested and the best fit has been considered for present analysis. These single variable regression models indicates the linear relationship exist between *ASFR* and relative flow depth β for all the channels with different width ratio (i.e., $\alpha = 3$ to 12). The best functional linear relationship of *ASFR* with β is $ASF = \mathrm{F}(\mathrm{A}\alpha + \mathrm{B})$. Similarly the prediction models for *ASFR* with respect to width ratio are also linear in form as indicated by *ASFR* = $\mathrm{F}(\mathrm{C}\alpha + \mathrm{D})$. The dependency of aspect ratio shows a exponential relationship and indicated by *ASFR* = $Ee^{n\delta}$ have been chosen for the modelling of *ASFR* where *A, B, C*, *D, E* and *n* are the functional coefficients. A multi variable regression model is attempted considering width ratio (α), relative depth (β), and aspect ratio (δ), resulting in three different single variable regression models. The final expression for *ASFR* is represented by

$$ASFR = P + Q\beta + R\alpha + Se^{n\delta} \tag{5}$$

Where *P, Q, R, S* and *n* are the functional coefficients with $P = 0.146$, $Q = -0.202$, $R = -0.01$ $S = 0.12$, $n = -0.05$. For finding out the apparent shear force directly the *ASFR* is multiplied with the total gravitational term ρgAS_0 and then represented by

$$ASF = \left(P + Q\beta + R\alpha + Se^{n\delta}\right)\rho gAS_0 \tag{6}$$

For predicting Discharge, first the area correction (ΔA) can be obtained from equation (7) andconsequently, the total discharge (Q) in the asymmetric compound channel is obtained from the equation (8)

$$\Delta A = \frac{ASF}{\rho g S_0} \quad \text{or} \quad \Delta A = \frac{\tau_{av} * h}{\rho g S_0} \tag{7}$$

$$Q = \frac{A_{mc} - \Delta A}{n_{mc}} R_{mc}^{\frac{2}{3}} S_0^{\frac{1}{2}} + \frac{A_f + \Delta A}{n_f} R_f^{\frac{2}{3}} S_0^{\frac{1}{2}} \tag{8}$$

Where: τ_{av} apparent shear stress, A_{mc} = Area of the main channel; R_{mc} = hydraulic radius; n_{mc} = Manning's roughness coefficient of the main channel; n_{fp} = Manning's roughness coefficient of the floodplain; $R_f = A_f / P_f$ = hydraulic radius of the section.

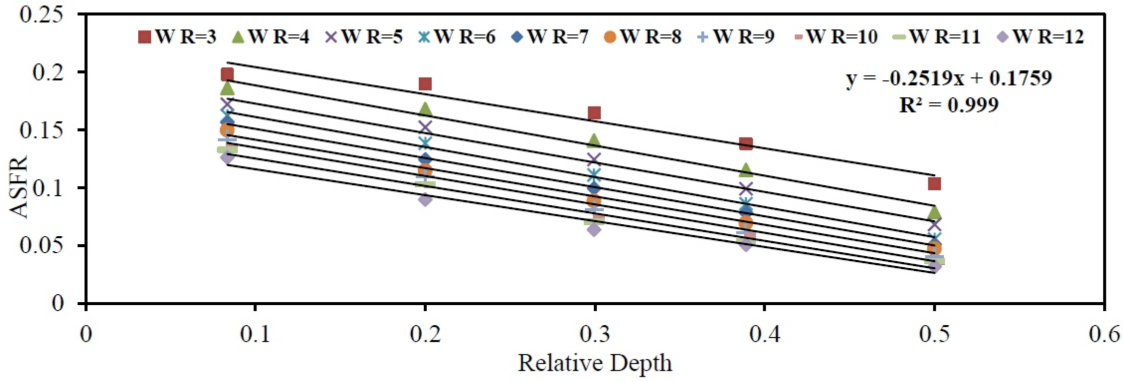

Figure4. Variation of *ASFR* with relative flow depth (Type 1)

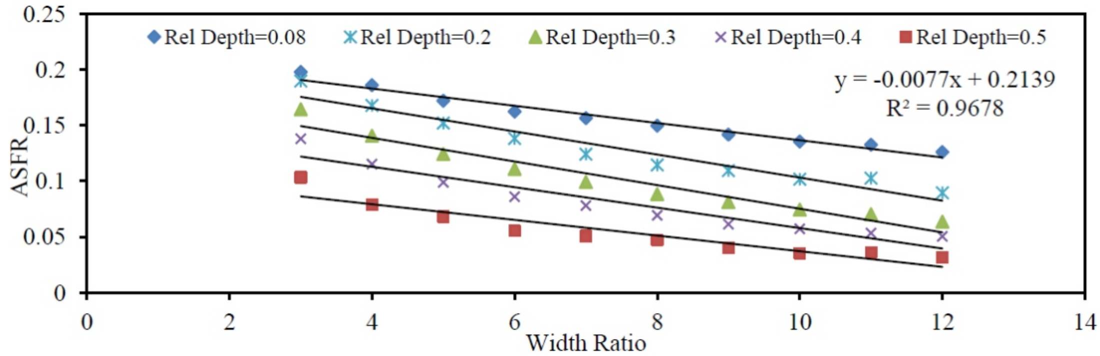

Figure 5. Variation of *ASFR* with width ratios for different relative flow depths (Type 1)

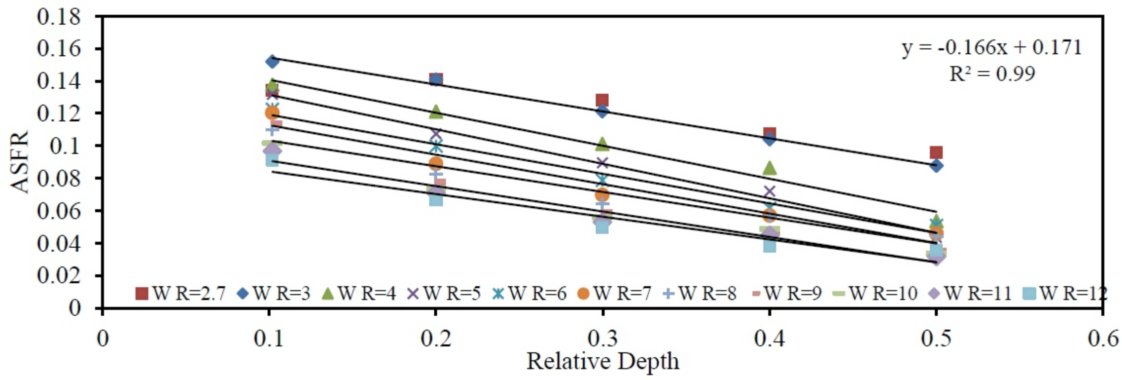

Figure 6. Variation of *ASFR*with relative flow depth (Type 2)

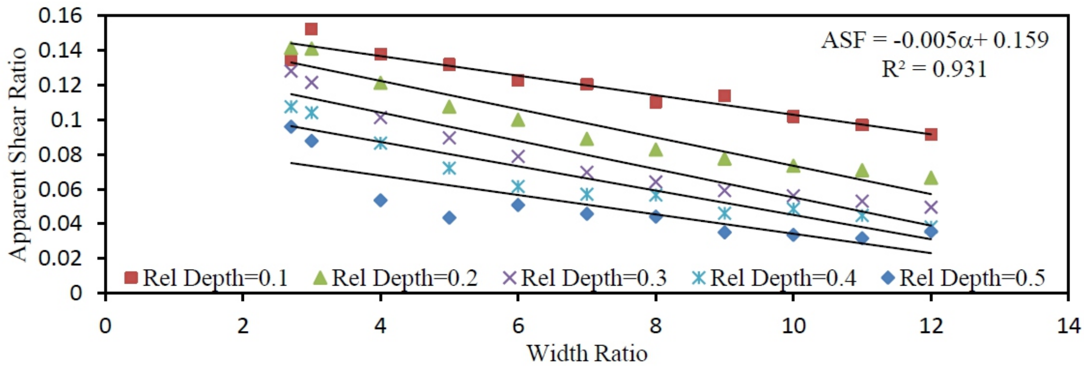

Figure 7. Variation of *ASFR*with width ratios for different relative flow depths(Type 2)

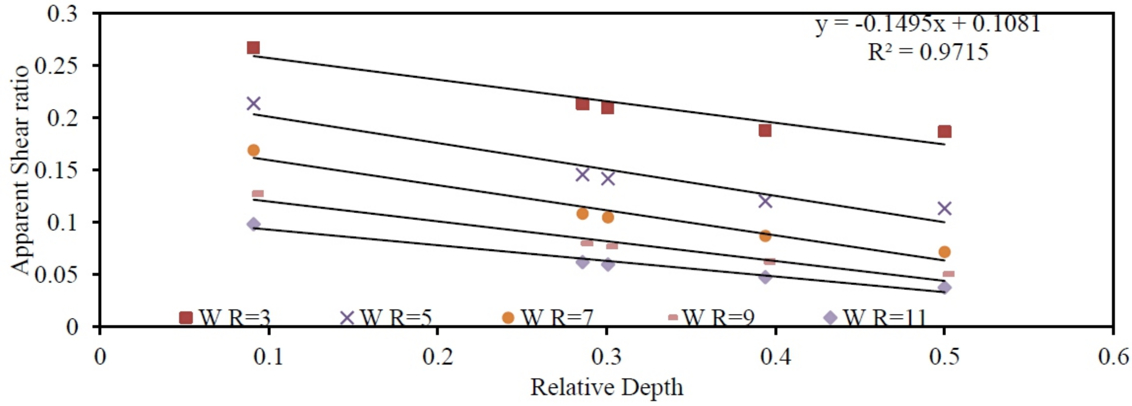

Figure 8. Variation of ASFRwith relative flow depths (Type 3)

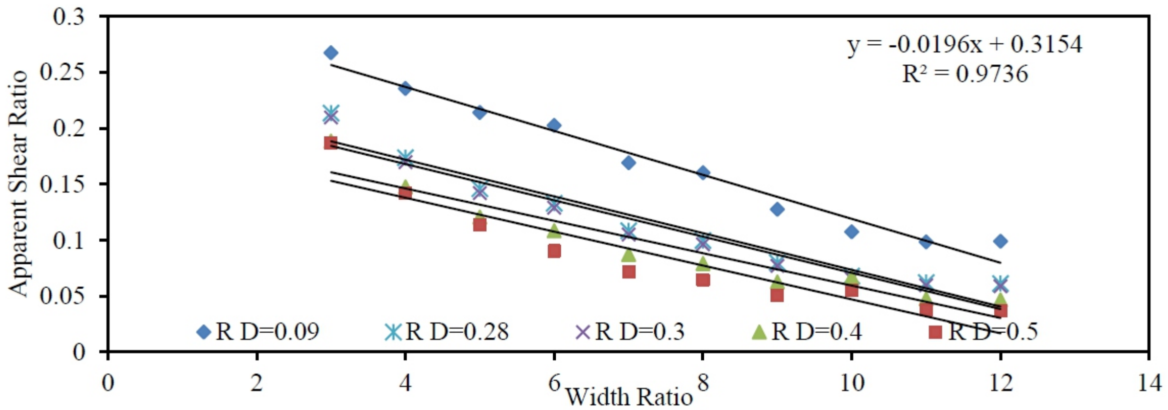

Figure 9. Variation of ASFR with width ratios for different relative flow depths (Type 3)

The apparent shear stress depends upon the aspect ratio of the main channel and found to increase with inverse of aspect ratio (z/b).(Ackers 1993, Moreta and Martin 2010). Moreta and Martin 2010 have demonstrated that for identical width ratio of compound channel and there is a large increase in apparent shear for changing aspect ratio from 2 to 8. Here Fig. 10 shows the reduction of *ASSR* with increase of aspect ratio.

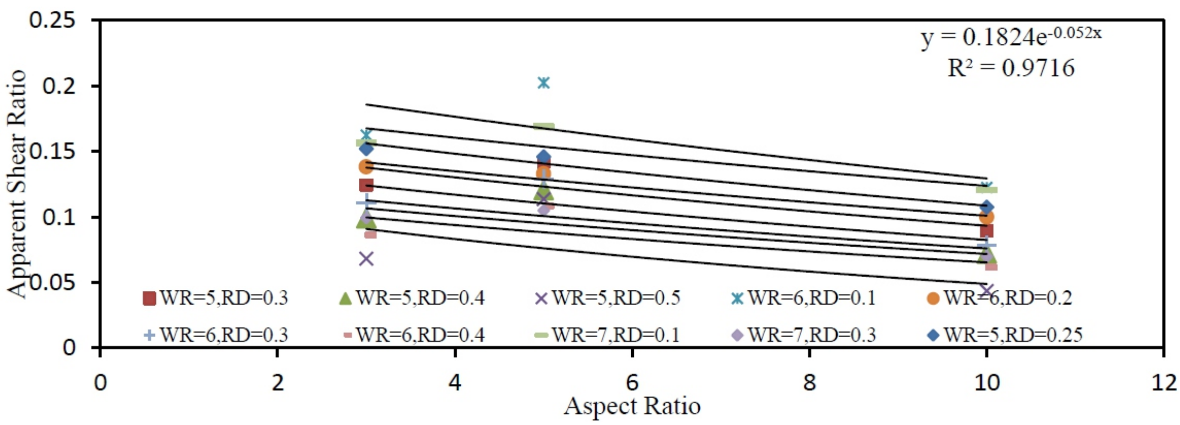

Figure 10. Variation of ASFR with aspect ratios for different relative flow depths

4.1 Comparison of different discharge prediction methods

Prinos (1984), Christodoulou (1992), Martin-Vide(2008), Khatua(2008) and many investigators have established that the apparent shear stress acting at the vertical interface depend primarily on width ratio (B/b) and the relative depth (h/H).There is always a clear dependence on the relative depth which has been observed for the apparent shear values as presented by previous investigators (e.g., Christodoulou and Myers (1999), Prinos and Townsend (1984), Khatua and Patra (2012). After formulation of the present expression it is compared with the other standard approaches. The standard approaches, considered are

1.Prinos (1984)

$$\tau_{av} = 0.874\left(\frac{h}{H}\right)^{1.129}\left(\frac{b_f}{b}\right)^{-.514}(\Delta V_v)^{.92} \tag{9}$$

2. Cristodoulou(1992)

$$\tau_{av} = 0.005\rho\left(\frac{B}{b}\right)^{-.514}(\Delta V_v)^2 \tag{10}$$

3. Martin-Vide(2008)

$$\tau_{av} = 0.002\rho\left(\frac{B}{b}\right)\left(\frac{2Z}{b}\right)^{-.514}\left(\frac{h}{H}\right)^{-\frac{1}{3}} * (\Delta V_v)^2 \tag{11}$$

4.Khatua(2008)

$$\Delta A = \left[\frac{\%S_f}{100} - \frac{(\alpha-1)\beta}{1+(\alpha-1)\beta}\right]A \tag{12}$$

Where $\%S_f$ is the percentage shear force given by

$$\%S_f = 3.4817\left[\frac{100(\alpha-1)\beta}{1+(\alpha-1)\beta}\right]^{.7317} \tag{13}$$

Where ΔV_v is the difference in velocities between main channel and flood plain with vertical interface as obtained from manning formula. α is the width ratio $\left[\frac{B}{b}\right]$, β is the relative depth $\left[\frac{h}{H}\right]$. Three experimental asymmetrical compound channel with aspect ratio 3, 5 and 10 available in literatures are considered for the validation. The equation (6) is an essentially improved model that takes into account of most influencing parameter such as width ratio, relative depth and aspect ratio.

First different regression-based models (Equation 9 to Equation13) as listed earlier have been compared with the developed (Equation6) method by applying to the asymmetrical compound channel of NITR, FCF and Khatibet al..(2013) for specific ranges of depths. This equations show the apparent shear stress (τ_{av})based on dimensionless parameter like width ratio, relative depth which are used to find out the area correction from equation(7) andthen the total discharge is evaluated from equation 8. The overview of these experimental data sets areprovided in Table 2.

Table 2. Geometric and hydraulic parameters of data sets

All Series	Bed Width(m)	Bank full Depth(m)	Side Slope	Bed Slope	Relative Depth	Aspect Ratio	Width Ratio	Manning's *n*
NITR	0.33	0.11	01:01	0.001325	0.043-0.27	3	5.1	0.01
FCF	1.5	0.15	01:01	0.001027	0.05- 0.5	10	2.7	0.01
Khatibet al.(2013)	0.1	0.02	–	0.0025	0.6-0.82	5	3	0.015
River Trent	15.4	2.1	01:05.2	0.001	0.032-0.12	7.33	5.14	0.032 & 0.015

The efficiency of each model is examined by calculating three types of errors for discharge prediction i.e., Mean percentage error (MPE), Mean absolute percentage error (MAPE) and Root mean square errors (RMSE) for different relative depths for these NITR, FCF and Khatibet al. 2013 as tabulated in Table 3(a), 3(b) and 3(c) respectively. From the error analysis, it is intriguing to note that the present approach appears to provide less error with reasonable accuracy. Then the average error in the discharge estimation was calculated for each test case as demonstrated in Figure11(a), 11(b) and 11(c), which cover a specific range of relative depths and expressed as a percentage.

The present model is found to be well matching with all data sets as compared to other methods and provides minimum 7% error for NITR channels, 2% error for FCF channel and 6% error for Khatib et al. 2013 channels as demonstrated in Figure 11(a), 11(b) and 11(c). Even when less error is found from Prinos (1984) model, they are not found suitable to provide accurate results for other two test cases (FCF, Khatib et al. 2013). Because,the discharge prediction from present model is either over or underestimated for each series, where the errors obtained from other models are inconsistent, so the MPE is high for present approach in NITR channels but MAPE is least than others.

The present model shows less error as compared to others because the proposed model is developed in asymmetric channels as they are for a likely range of relative flow depths ($\beta = 0.1\text{-}0.5$) to be encountered in practice. But below this range the magnitude of errors increases. Khatua(2008) model shows less error for FCF channels but fails to provide better results for Khatibet al.(2013)channel as this model is developed for higher width ratio but the width ratio of the Khatib's channel is 3 and this model established for rectangular and trapezoidal channels.

Table3(a) Computed MPE, MAPE and RMSE for five discharge models in NITR Series

Method	MPE	MAPE	RMSE
Model	10.10	6.53	0.03
Prinos	3.00	3.97	0.01
Cristodoulou	19.27	19.27	0.04
Martin-Vide	21.80	21.80	0.05
Khatua	15.29	15.29	0.02

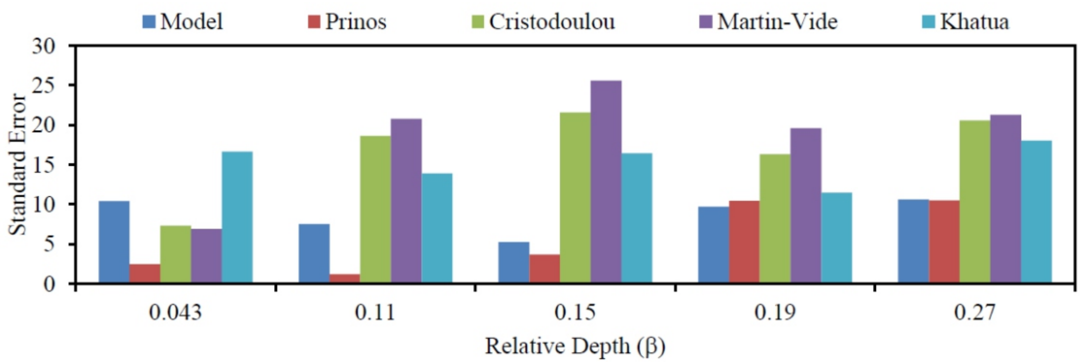

Figure 11 (a) Variation of standard error of discharge for various models in NITR

Table 3(b) Computed MPE, MAPE and RMSE for five discharge models in FCF Series

Method	MPE	MAPE	RMSE
Model	-3.74	2.64	0.02
Prinos	-3.62	4.48	0.05
Cristodoulou	2.03	4.62	0.05
Martin-Vide	2.55	4.30	0.05
Khatua	2.78	3.64	0.02

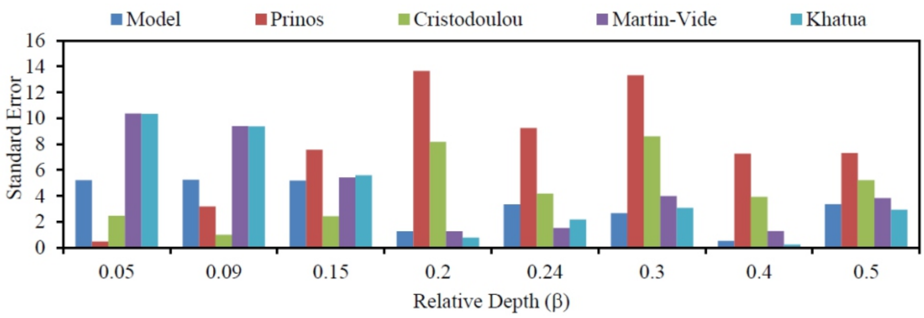

Figure11 (b) Variation of standard error of discharge for various models in FCF Series 6

Table 3(c) Computed MPE, MAPE and RMSE for five discharge models in Khatib et al.(2013) Series

Method	MPE	MAPE	RMSE
Model	-5.56	5.83	0.35
Prinos	-7.45	7.77	0.51
Cristodoulou	-7.53	7.81	0.51
Martin-Vide	-7.46	7.76	0.20
Khatua	-11.25	11.38	0.57

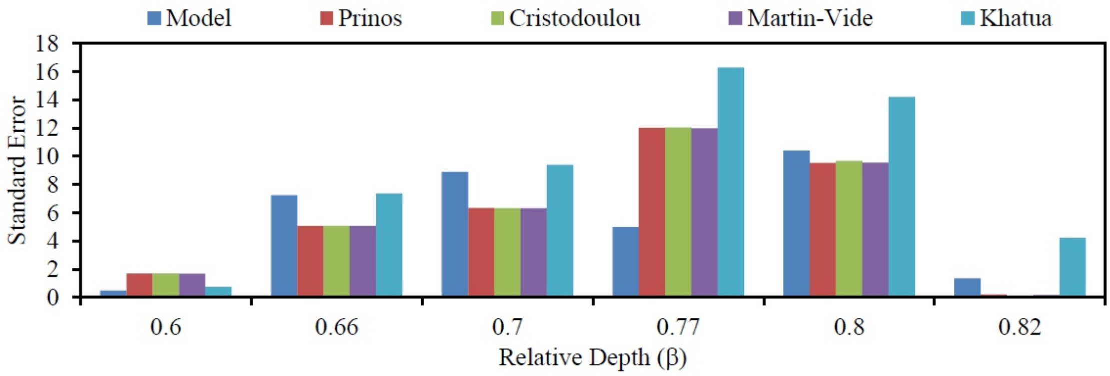

Figure 11 (c) Variation of standard error of discharge for various models in Khatib et al.(2013) Series

4.2 Application of field data

The approach is also successfully evaluated in predicting the discharge in a natural river Trent, UK. The results of field measurements of cross sectional geometry have been presented in Figure. 12. The river Main, considered for study has almost straight, uniformcross section and trapezoidal shape of the main channel. For analysis, the shape has been finalised in such a way that the total cross sectional area and wetted perimeter of the reach remain unchanged as compared to the original geometry as shown in Figure 12. The overview of this natural river data are provided in Table 2. The outputs of the errors of discharge values has been analysed for the river cross section for seven over bank flow depths using all the approaches. The present approach is found to give consistent errors for lower and higher flow depthwith minimum error up to 4.84% on the other hand the results of Khatua(2008) model demonstrates maximum errors for low relative flow depths and less error for high relative flow depths. Other three methods are seen to provide better results for low relative depth and give high difference in accuracies for larger depth of flowas these methods have been derived solely for symmetrical compound channels where as the present approach has been derived for asymmetrical compound channels. The error results in terms of MPE, MAPE and RMSE are given in Table 4. The new method is found to have the least RMSE in discharge estimation thus offers an alternative methodology for satisfactory predicting the dischargein all cases.

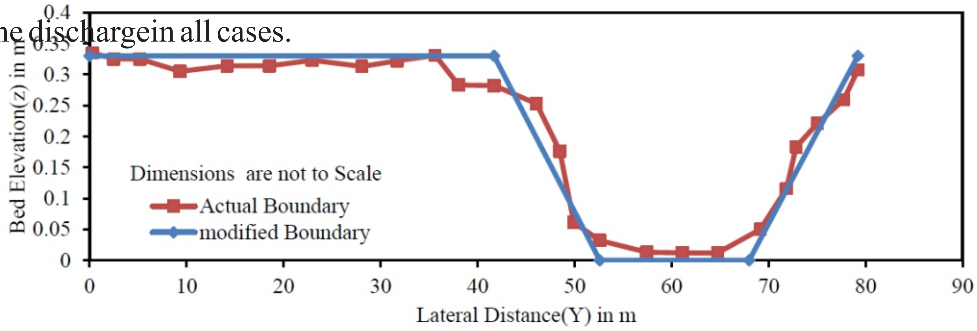

Table 4. Computed MPE, MAPE and RMSE for seven discharge models in river Trent, UK

Method	MPE	MAPE	RMSE
Model	4.84	4.84	0.07
Prinos	6.33	6.33	0.08
Cristodoulou	6.03	6.03	0.07
Martin-Vide	5.86	5.86	0.07
Khatua	10.44	10.44	0.11

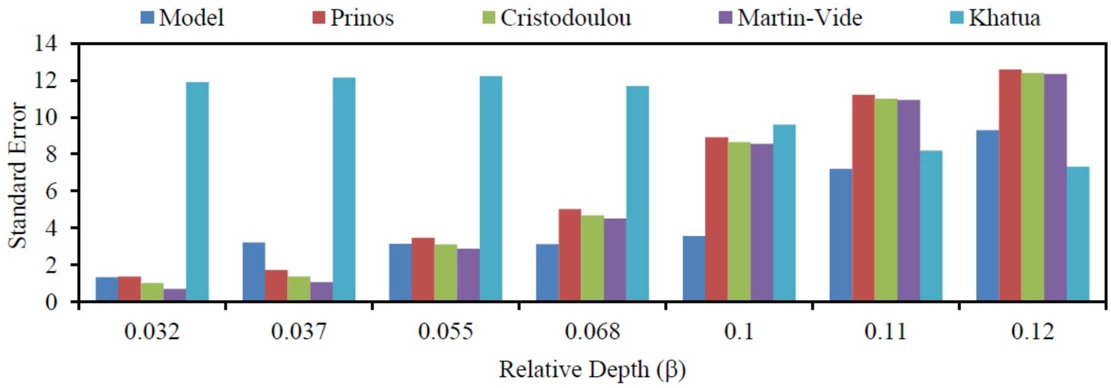

Figure 13. Variation of standard error of discharge for various models in river Trent, UK

5. Conclusions

The following conclusions can be drawn from the above experimental and numerical investigation

Thenumerical method SKM which is based on the simplification of Navier Stokes equation has been found to provide most accurate boundary shear distribution results, So in present work this technique has been successfully utilised to generate the wide ranges of datasets of boundary shear stress distribution of compound channels which in turns helpful for evaluating the apparent shear stress.

The apparent shear stress ratios of asymmetric compound channels are found to increase with decrease of aspect ratio. The apparent shear stress ratio are also found to decrease with increase of the over bank flow depths and with width ratio.

The previous approaches presented by the previous investigators are found to be not suitable for predicting apparent shear stress in an asymmetric compound channel due to improper consideration of interaction mechanism.

A multilinear regression model for predicting apparent shear has been developed by taking care of the dependency of ASF with non dimensional parameters like only. The proposed model on the basis of new expression of apparent shear ratio for prediction of discharge in a compound channel is found to give very less error as compared to results from previous investigators. As the method is able to predict the discharge with least errors for both experimental and river data, it is hoped this new expression will be useful for satisfactorily estimate the discharge in laboratory and field.

References

- *Ackers, P. (1993). Flow formulae for straight two-stage channels. Journal of Hydraulic Research, 31(4), 509-531.*
- *Al-Khatib, I. A., Dweik, A. A., &Gogus, M. (2012).Evaluation of separate channel methods for discharge computation in asymmetric compound channels. Flow Measurement and Instrumentation, 24, 19-25.*
- *Al-Khatib, I. A., Hassan, H. A., & Abaza, K. A. (2013).Application and validation of regression analysis in the prediction of discharge in asymmetric compound channels. Journal of Irrigation and Drainage Engineering, 139(7), 542-550.*
- *Christodolou, G. C., & Myers, W. R. C. (1999).Apparent friction factor on the flood plain-main channel interface of compound channel sections. InProceedings of 28th Congress of the International Association for Hydraulic Research.*
- *Garcia, J. L., Perez-Caro, M., Gomez-Moreta, J. A., Gonzalez, F., Ortiz, J., Blanco, O., ...& Sanchez-Martin, M. (2010). Molecular analysis of ex-vivo CD133+ GBM cells revealed a common invasive and angiogenic profile but different proliferative signatures among high grade gliomas. BMC cancer, 10(1), 454.*

- *Garcia, J. L., Perez-Caro, M., Gomez-Moreta, J. A., Gonzalez, F., Ortiz, J., Blanco, O., ...& Sanchez-Martin, M. (2010). Molecular analysis of ex-vivo CD133+ GBM cells revealed a common invasive and angiogenic profile but different proliferative signatures among high grade gliomas. BMC cancer, 10(1), 454.*

- *Ghosh, S., & Jena, S. B. (1971, August).Boundary shear distribution in open channel compound. In ICE Proceedings (Vol. 49, No. 4, pp. 417-430). Thomas Telford.*
- *Günaydin, M., Sierra, G., & Townsend, P. K. (1984). The geometry of N= 2 Maxwell-Einstein supergravity and Jordan algebras. Nuclear Physics B, 242(1), 244-268.*
- *Khatua, K. K., & Patra, K. C. (2008).Interaction of Flow in Meandering and Straight Channel with Floodplains.*
- *Khatua, K. K., Patra, K. C., &Mohanty, P. K. (2011). Stage-discharge prediction for straight and smooth compound channels with wide floodplains. Journal of Hydraulic Engineering, 138(1), 93-99.*
- *Khatua, K. K., Patra, K. C., &Nayak, P. (2012).Meandering effect for evaluation of roughness coefficients in open channel flow 6th intern conf. on river basin management. WIT Transactions on Ecology and the Environment (ISSN 1743-3541), CMEM, and WIT Press, 146(6), 213-227.*

- *Khatua, K. K., Patra, K. C., &Nayak, P. (2012).Meandering effect for evaluation of roughness coefficients in open channel flow 6th intern conf. on river basin management. WIT Transactions on Ecology and the Environment (ISSN 1743-3541), CMEM, and WIT Press, 146(6), 213-227.*

- *Knight, D. W., &Demetriou, J. D. (1983). Flood plain and main channel flow interaction. Journal of Hydraulic Engineering, 109(8), 1073-1092.*
- *Knight, D. W., &Hamed, M. E. (1984).Boundary shear in symmetrical compound channels. Journal of Hydraulic Engineering.*
- *Knight, D. W., &Hamed, M. E. (1984).Boundary shear in symmetrical compound channels.Journal of Hydraulic Engineering*
- *Knight, D. W., Shiono, K., &Pirt, J. (1989, September).Prediction of depth mean velocity and discharge in natural rivers with overbank flow. InProceedings of the International Conference on Hydraulic and Environmental Modellling of Coastal, Estuarine and River Waters (pp. 419-428).*
- *Lopez-Bustins, J. A., Martin-Vide, J., & Sanchez-Lorenzo, A. (2008). Iberia winter rainfall trends based upon changes in teleconnection and circulation patterns. Global and Planetary Change, 63(2), 171-176.*
- *Myers, S. C. (1977). Determinants of corporate borrowing. Journal of financial economics, 5(2), 147-175.*
- *Patra, K. C., &Kar, S. K. (2000). Flow interaction of meandering river with floodplains. Journal of Hydraulic Engineering, 126(8), 593-604.*

- *Patra, K. C., & Khatua, K. K. (2006, September).Selection of Interface Plane in the Assessment of Discharge in Two Stage Meandering and Straight Compound Channels. In River Flow 2006, Two Volume Set: Proceedings of the International Conference on Fluvial Hydraulics, Lisbon, Portugal, 6-8 September 2006 (Vol. 1, p. 379). CRC Press.*
- *Prinos, P., & Townsend, R. D. (1984).Comparison of methods for predicting discharge in compound open channels. Advances in water resources, 7(4), 180-187.*
- *Prinos, P., & Townsend, R. D. (1984).Comparison of methods for predicting discharge in compound open channels. Advances in water resources, 7(4), 180-187.*
- *Rajaratnam, N., & Ahmadi, R. M. (1979).Interaction between main channel and flood-plain flows. Journal of the Hydraulics Division, 105(5), 573-588.*
- *Sellin, T., & Wolfgang, M. E. (1964).The measurement of delinquency.*
- *Tatuch, Y., Christodoulou, J., Feigenbaum, A., Clarke, J. T., Wherret, J., Smith, C., ...& Robinson, B. H. (1992). HeteroplasmicmtDNA mutation (T----G) at 8993 can cause Leigh disease when the percentage of abnormal mtDNA is high. American journal of human genetics, 50(4), 852.*
- *Weber, J. F., & Menéndez, A. N. (2004, June). Performance of lateral velocity distribution models for compound channel sections. In Proceedings of international conference on fluvial hydraulics of river flow (Vol. 1, pp. 449-57).*
- *Wilkinson, A., Marchington, M., Goodman, J., & Ackers, P. (1992). Total quality management and employee involvement. Human Resource Management Journal, 2(4), 1-20.*
- *Wormleaton, P. R., Allen, J., &Hadjipanos, P. (1982). Discharge assessment in compound channel flow. Journal of the Hydraulics Division, 108(9), 975-994.*
- *Wright, R. R., &Carstens, M. R. (1970).Linear-momentum flux to overbank sections. Journal of the Hydraulics Division, 96(9), 1781-1793.*

Instructions for Authors

Essentials for Publishing in this Journal

1 Submitted articles should not have been previously published or be currently under consideration for publication elsewhere.

2 Conference papers may only be submitted if the paper has been completely re-written (taken to mean more than 50%) and the author has cleared any necessary permission with the copyright owner if it has been previously copyrighted.

3 All our articles are refereed through a double-blind process.

4 All authors must declare they have read and agreed to the content of the submitted article and must sign a declaration correspond to the originality of the article.

Submission Process

All articles for this journal must be submitted using our online submissions system. http://enrichedpub.com/ . Please use the Submit Your Article link in the Author Service area.

Manuscript Guidelines

The instructions to authors about the article preparation for publication in the Manuscripts are submitted online, through the e-Ur (Electronic editing) system, developed by **Enriched Publications Pvt. Ltd**. The article should contain the abstract with keywords, introduction, body, conclusion, references and the summary in English language (without heading and subheading enumeration). The article length should not exceed 16 pages of A4 paper format.

Title

The title should be informative. It is in both Journal's and author's best interest to use terms suitable. For indexing and word search. If there are no such terms in the title, the author is strongly advised to add a subtitle. The title should be given in English as well. The titles precede the abstract and the summary in an appropriate language.

Letterhead Title

The letterhead title is given at a top of each page for easier identification of article copies in an Electronic form in particular. It contains the author's surname and first name initial .article title, journal title and collation (year, volume, and issue, first and last page). The journal and article titles can be given in a shortened form.

Author's Name

Full name(s) of author(s) should be used. It is advisable to give the middle initial. Names are given in their original form.

Contact Details

The postal address or the e-mail address of the author (usually of the first one if there are more Authors) is given in the footnote at the bottom of the first page.

Type of Articles

Classification of articles is a duty of the editorial staff and is of special importance. Referees and the members of the editorial staff, or section editors, can propose a category, but the editor-in-chief has the sole responsibility for their classification. Journal articles are classified as follows:

Scientific articles:

1. Original scientific paper (giving the previously unpublished results of the author's own research based on management methods).
2. Survey paper (giving an original, detailed and critical view of a research problem or an area to which the author has made a contribution visible through his self-citation);
3. Short or preliminary communication (original management paper of full format but of a smaller extent or of a preliminary character);
4. Scientific critique or forum (discussion on a particular scientific topic, based exclusively on management argumentation) and commentaries. Exceptionally, in particular areas, a scientific paper in the Journal can be in a form of a monograph or a critical edition of scientific data (historical, archival, lexicographic, bibliographic, data survey, etc.) which were unknown or hardly accessible for scientific research.

Professional articles:

1. Professional paper (contribution offering experience useful for improvement of professional practice but not necessarily based on scientific methods);
2. Informative contribution (editorial, commentary, etc.);
3. Review (of a book, software, case study, scientific event, etc.)

Language

The article should be in English. The grammar and style of the article should be of good quality. The systematized text should be without abbreviations (except standard ones). All measurements must be in SI units. The sequence of formulae is denoted in Arabic numerals in parentheses on the right-hand side.

Abstract and Summary

An abstract is a concise informative presentation of the article content for fast and accurate Evaluation of its relevance. It is both in the Editorial Office's and the author's best interest for an abstract to contain terms often used for indexing and article search. The abstract describes the purpose of the study and the methods, outlines the findings and state the conclusions. A 100- to 250-Word abstract should be placed between the title and the keywords with the body text to follow. Besides an abstract are advised to have a summary in English, at the end of the article, after the Reference list. The summary should be structured and long up to 1/10 of the article length (it is more extensive than the abstract).

Keywords

Keywords are terms or phrases showing adequately the article content for indexing and search purposes. They should be allocated heaving in mind widely accepted international sources (index, dictionary or thesaurus), such as the Web of Science keyword list for science in general. The higher their usage frequency is the better. Up to 10 keywords immediately follow the abstract and the summary, in respective languages.

Acknowledgements

The name and the number of the project or programmed within which the article was realized is given in a separate note at the bottom of the first page together with the name of the institution which financially supported the project or programmed.

Tables and Illustrations

All the captions should be in the original language as well as in English, together with the texts in illustrations if possible. Tables are typed in the same style as the text and are denoted by numerals at the top. Photographs and drawings, placed appropriately in the text, should be clear, precise and suitable for reproduction. Drawings should be created in Word or Corel.

Citation in the Text

Citation in the text must be uniform. When citing references in the text, use the reference number set in square brackets from the Reference list at the end of the article.

Footnotes

Footnotes are given at the bottom of the page with the text they refer to. They can contain less relevant details, additional explanations or used sources (e.g. scientific material, manuals). They cannot replace the cited literature.
The article should be accompanied with a cover letter with the information about the author(s): surname, middle initial, first name, and citizen personal number, rank, title, e-mail address, and affiliation address, home address including municipality, phone number in the office and at home (or a mobile phone number). The cover letter should state the type of the article and tell which illustrations are original and which are not.

Notes: